2-10-2015

Material Biocompatibility and Applications in Metabolic Monitoring

Michail Kastellorizios
University of Connecticut - Storrs, michalis108@gmail.com

Material Biocompatibility and Applications in Metabolic Monitoring

Michail Kastellorizios, PhD

University of Connecticut, 2015

The present dissertation focuses and expands on the optimization and application of poly(lactic-co-glycolic acid) (PLGA)/polyvinyl alcohol (PVA) composite coatings and initiates metabolic studies in small animals to identify novel biomarkers to be utilized in exhaustion prediction. The composites are used to coat implantable biosensors and improve their biocompatibility. The objectives of the work are: *i)* investigate species differences related to the foreign body reaction (FBR) between small and large animals; *ii)* develop composite coatings to prevent the FBR in large animals; *iii)* develop composites loaded with combinations of dexamethasone, vascular endothelial growth factor (VEGF) and platelet derived growth factor (PDGF) to promote angiogenesis around implanted biosensors; and *iv)* apply multi-analyte monitoring to exhaustion prediction.

The onset and severity of fibrosis was identified as a key difference between minipigs and rats, with minipigs demonstrating earlier onset and more severe chronic inflammation. In order to counter this, dexamethasone release must be continuous, with no lag phase. The effective dexamethasone dosing regime was 100 μg during the first day and 10 μg/day thereafter.

A novel method for the preparation of microspheres containing insoluble drugs was developed to achieve homogeneous drug distribution, high loading and low burst release. Dexamethasone microspheres prepared by this method were utilized in microsphere/hydrogel composite coatings which successfully prevented FBR in a large animal model for a period of one month.

Combinations of dexamethasone, VEGF and PDGF were investigated for the first time to prevent FBR and promote angiogenesis. It was determined that VEGF has to be delivered at higher doses than PDGF and an increase in dexamethasone must be accompanied by proportional increase in growth factors.

An array of biomarkers that can be used in exhaustion prediction was successfully identified, with prediction times ranging from 10 to 20 minutes in normal as well as type 1 diabetic rats. It was discovered that multi-analyte biomarkers based on glucose and lactate are far more responsive in the subcutaneous tissue (an implantation-friendly compartment) than in the blood.

In conclusion, the outcomes of this work contribute to the advancement biomaterials, as well as applications in exercise physiology.

Material Biocompatibility and Applications in Metabolic Monitoring

Michail Kastellorizios

B.Pharm., University of Patras, 2008

M.Sc., University of Patras, 2010

A Dissertation

Submitted in Partial Fulfillment of the

Requirements for the Degree of

Doctor of Philosophy

at the

University of Connecticut

2015

APPROVAL PAGE

Doctor of Philosophy Dissertation

'Material Biocompatibility and Applications in Metabolic Monitoring'

Presented by

Michail Kastellorizios, B.Pharm., M.Sc.

Major Advisor

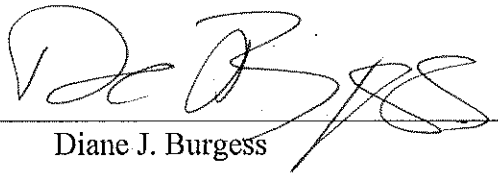

Diane J. Burgess

Associate Advisor

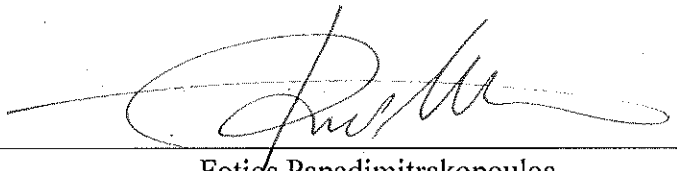

Fotios Papadimitrakopoulos

Associate Advisor

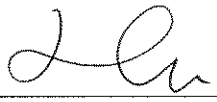

Xiuling Lu

University of Connecticut
2015

Acknowledgements

I would like to express my sincere appreciation to my advisor Dr. Diane J. Burgess. You are the best mentor that a new scientist can hope for, and I will always be grateful for the encouragement I received to pursue my research interests. Your advice has proven invaluable for my research as well as my career. Thanks to your mentorship I learned the importance of multi-disciplinary approaches, critical thinking and hard work, and developed professional, leadership, and team-building skills. Thank you for your patience and the hard work that you dedicated to me, and I sincerely hope that our professional and personal relationship will last and grow.

A special thanks to Dr. Fotios Papadimitrakopoulos, my associate advisor, for his continuing support, advice, and his efforts to sustain a multi-disciplinary project which I was fortunate to be part of. I am also very thankful to Dr. Xiuling Lu, my associate advisor, for her advice and the time she dedicated to my work.

I am deeply thankful to the Pharmaceutics faculty members Dr. Michael Pikal, Dr. Devendra Kalonia, Dr. Robin Bogner, and Dr. Bodhi Chaudhuri for the exceptional coursework and scientific input, Dr. Faquir Jain for his collaboration and to Dr. David Grant for allowing me to use instruments in his laboratory. I am grateful for the immense help I received from the School of Pharmacy administrative personnel, especially from Ms. Leslie Lebel, Mr. Mark Armati, Ms. Laura Burnett, Ms. Kathleen Koji, Ms. Mina Boone and Ms. Jacqueline Maliga.

I would like to thank all past and present project collaborators and lab members, especially Dr. Sagar Vaddiraju, Dr. Yan Wang, Ms. Namita Tipnis, Mr. Bing Gu, Dr. Jie Shen, Dr. Robert Croce, Mr. Allen Legassey, Mr. Nanda Kommineni, Ms. Claire Price, Dr. Jacqueline Morais, Dr. Sudhir Verma, Dr. Archana Rawat, Dr. Xiaoming Xu, Dr. Sumit Kumar, Dr. Nitin Swarnakar, Mr. Antonio Costa, Mr. Minsung Suh, Mr. Rajan Jog, Ms. Janki Andhariya, Ms. Carmen Zhang, and everyone else who offered me their help and friendship.

This work would not have been possible without the help and support from UConn's Animal Care Services, the Institutional Animal Care and Use Committee and the attending veterinarian Dr. Cecile Baccanale who helped me ensure that all animal studies were performed with utmost respect to animal life. A very special thanks to Ms. Janet Trombley who went out of her way time and again to help me with the care, enrichment and experimental aspects of the minipig studies presented here. I will never forget your help.

I would like to acknowledge the financial support I received from the United States Department of Defense for my research projects and the University of Connecticut for the assistantships and tuition waivers.

Lastly, I would never have reached this point without the love and support from my parents, Georgios Kastellorizios and Theodora Lakata, my brother Nikolaos Kastellorizios, my extended family and friends, and of course my spiritual guide and inspiration Shri Mataji Nirmala Devi.

Table of Contents

Appendix II - Tables

Chapter 1

Introduction

1.1. Background

Diabetes mellitus[1-3], obesity[4-9], metabolic syndrome[8, 10-15] and intense physical activity[16-19] are a few examples of conditions whose management requires close monitoring of their progress and status. Typically, this takes place *via* monitoring of the overall physical condition of the individual (weight, weight fluctuations, routine blood/urine tests, *etc.*). In addition to routine health screening, monitoring of condition-specific biomarkers is essential for adequate management as well as prevention in high-risk populations. For example, blood pressure and lipid content are periodically checked in patients with metabolic syndrome or those at risk of developing metabolic syndrome such as the obese.

Glucose, the main energy source in the body, has been identified as one of the most informative metabolic biomarkers regardless of the metabolic condition being treated. Fasting glucose[20-24] and the oral glucose tolerance test (OGTT)[25-30] are two tests run routinely (typically on a semi-annual or quarterly basis) to pick up metabolic abnormalities. Diabetic patients require more frequent glucose monitoring (multi-daily) in order to account for pre-meal blood glucose concentrations when deciding the dose of insulin to be injected and/or the type and amount of food to be consumed. However, the aforementioned glucose tests and monitoring regimes can only give discreet values of glucose levels; they do not provide glucose trends (increasing or decreasing) or glucose fluctuations between measurements. As a result, managing the metabolic condition becomes a daily struggle for patients who are required to be on alert 24/7 and take important decisions on insulin (a very toxic drug) dosing. Accordingly, continuous glucose monitoring is necessary for the successful management of metabolic diseases, particularly diabetes.

Previous research has provided competitive solutions towards the realization of a fully implantable metabolic biosensor regarding the four major challenges surrounding metabolic

monitoring: *i)* long-term biosensor functionality in the body; *ii)* sensitivity and response linearity of multi-analyte biosensors; *iii)* miniaturization and wireless communications; and *iv)* interpretation of metabolic data and identification of monitoring biomarkers. This has resulted in: *a)* subcutaneously-implanted multi-analyte biosensors with superior sensitivity and response linearity in rats[31, 32]; *b)* miniaturized electrical circuits and wireless communication and power supply platforms[33]; and *c)* composite biosensor coatings that suppress the body's reaction to implanted biosensors for three months in rats[34-38].

The biosensor coatings presented here are made of poly(lactic-co-glycolic acid) (PLGA) microspheres embedded in a polyvinyl alcohol (PVA) hydrogel. The PVA hydrogel acts as base for the coating that allows glucose and other analytes to diffuse from the local microenvironment to the biosensor. In addition, PVA-based hydrogels have mechanical properties similar to that of soft tissues such as the subcutaneous tissue; this ensures that the implant will not cause tissue trauma. The PLGA microspheres serve as drug depots that release dexamethasone, a synthetic glucocorticosteroid with immunosuppressant and anti-inflammatory action. Dexamethasone was chosen due to its high potency that allows suppression of the foreign body response (FBR) with small amounts of drug, a necessity resulting from the small size of the biosensors. The PLGA microsphere/PVA hydrogel coatings have been tested in small animals (rats) to optimize the dexamethasone dose and release kinetics. Our group has successfully tested a first generation of semi-implantable coated glucose biosensors in rats that maintained functionality for one month.

In addition to dexamethasone, vascular endothelial growth factor (VEGF) has been incorporated in the PLGA/PVA coatings to induce angiogenesis, the sprouting of blood vessels[39]. Continuous release of VEGF from the PLGA microspheres into the subcutaneous tissue microenvironment has offset the dexamethasone-induced ischemia observed in dexamethasone-

only coatings. Adequate perfusion (amount of blood volume) at the biosensor microenvironment is essential to ensure rapid transfer of blood glucose to the subcutaneous tissue, to be quantified by the implanted biosensor with minimal lag time.

1.2. Objectives

The present dissertation focuses and expands on the optimization and application of poly(lactic-co-glycolic acid) (PLGA)/polyvinyl alcohol (PVA) composite coatings and initiates metabolic studies in small animals to identify novel biomarkers to be utilized in exhaustion prediction. These composites are used to coat implantable biosensors and improve their biocompatibility. The objectives of the work are: *i)* investigate species differences related to the foreign body reaction (FBR) between small and large animals; *ii)* develop composite coatings to prevent the FBR in large animals; *iii)* develop composites loaded with combinations of dexamethasone, vascular endothelial growth factor (VEGF) and platelet derived growth factor (PDGF) to promote angiogenesis around implanted biosensors; and *iv)* apply multi-analyte monitoring for exhaustion prediction.

The work was divided into four Specific Aims:

SA-I Prevention of the foreign body reaction in a pre-clinical large animal model: inter-species differences

SA-II Development of dexamethasone-loaded PLGA microspheres for long-term prevention of the foreign body reaction in Gottingen minipigs

SA-III Delivery of dexamethasone, VEGF, and PDGF to promote angiogenesis and prevent the foreign body reaction in subcutaneous implants

SA-IV Continuous metabolic monitoring based on multi-analyte biomarkers to predict exhaustion

1.3. References

1. Miller, C.K., M.D. Gutschall, and C. Holloman, *Self-monitoring predicts change in fiber intake and weight loss in adults with diabetes following an intervention regarding the glycemic index.* Patient Educ Couns, 2009. **76**(2): p. 213-9.
2. Virdi, N.S., et al., *Association of self-monitoring of blood glucose use on glycated hemoglobin and weight in newly diagnosed, insulin-naive adult patients with type 2 diabetes.* J Diabetes Sci Technol, 2013. **7**(5): p. 1229-42.
3. Zhang, D.A., L. Katznelson, and M. Li, *Postprandial glucose monitoring further improved glycemia, lipids, and weight in persons with type 2 diabetes mellitus who had already reached hemoglobin A1c goal.* J Diabetes Sci Technol, 2012. **6**(2): p. 289-93.
4. Dickerson, R.N. and J.W. Drover, *Monitoring nutrition therapy in the critically ill patient with obesity.* JPEN J Parenter Enteral Nutr, 2011. **35**(5 Suppl): p. 44S-51S.
5. Eguchi, K., *Ambulatory blood pressure monitoring in diabetes and obesity-a review.* Int J Hypertens, 2011. **2011**: p. 954757.
6. El Awwa, A., et al., *Continuous glucose monitoring, oral glucose tolerance, and insulin - glucose parameters in adolescents with simple obesity.* Georgian Med News, 2012(210): p. 47-53.
7. Fallahi Khoshknab, M., et al., *The effect of weight monitoring and recording on control of obesity and overweight.* Eat Weight Disord, 2011. **16**(2): p. e137-41.
8. Kang, I.S., et al., *Association between Central Obesity and Circadian Parameters of Blood Pressure from the Korean Ambulatory Blood Pressure Monitoring Registry: Kor-ABP Registry.* J Korean Med Sci, 2013. **28**(10): p. 1461-7.
9. Neal Davis, R., et al., *Adolescent obesity and maternal and paternal sensitivity and monitoring.* Int J Pediatr Obes, 2011. **6**(2-2): p. e457-63.
10. Aldo Ferrara, L., et al., *Blood pressure at rest, during 24 h monitoring and in response to sympathetic stimulation in hypertensive patients with metabolic syndrome.* Int J Cardiol, 2007. **117**(3): p. 312-6.
11. Buscemi, S., et al., *Glycaemic variability using continuous glucose monitoring and endothelial function in the metabolic syndrome and in Type 2 diabetes.* Diabet Med, 2010. **27**(8): p. 872-8.
12. Hasnain, M., et al., *Clinical monitoring and management of the metabolic syndrome in patients receiving atypical antipsychotic medications.* Prim Care Diabetes, 2009. **3**(1): p. 5-15.
13. Khatana, S.A., et al., *Monitoring and prevalence rates of metabolic syndrome in military veterans with serious mental illness.* PLoS One, 2011. **6**(4): p. e19298.
14. Stuckey, M., et al., *Remote monitoring technologies for the prevention of metabolic syndrome: the Diabetes and Technology for Increased Activity (DaTA) study.* J Diabetes Sci Technol, 2011. **5**(4): p. 936-44.
15. Stuckey, M., et al., *Diabetes and Technology for Increased Activity (DaTA) study: results of a remote monitoring intervention for prevention of metabolic syndrome.* J Diabetes Sci Technol, 2011. **5**(4): p. 928-35.
16. Ren, J., A. Dean Sherry, and C.R. Malloy, *Noninvasive monitoring of lactate dynamics in human forearm muscle after exhaustive exercise by (1) H-magnetic resonance spectroscopy at 7 tesla.* Magn Reson Med, 2012.
17. Burkow-Heikkinen, L., *Non-invasive physiological monitoring of exercise and fitness.* Neurol Res, 2011. **33**(1): p. 3-17.
18. Bartels, S.A., et al., *Noninvasive cardiac output monitoring during exercise testing: Nexfin pulse contour analysis compared to an inert gas rebreathing method and respired gas analysis.* J Clin Monit Comput, 2011. **25**(5): p. 315-21.

19. Beckmann, L., et al., *Monitoring change of body fluids during physical exercise using bioimpedance spectroscopy.* Conf Proc IEEE Eng Med Biol Soc, 2009. **2009**: p. 4465-8.
20. Zhuo, X., et al., *Cost-Effectiveness of Alternative Thresholds of the Fasting Plasma Glucose Test to Identify the Target Population for Type 2 Diabetes Prevention in Adults Aged >=45 Years.* Diabetes Care, 2013.
21. Poomalar, G.K. and V. Rangaswamy, *A comparison of fasting plasma glucose and glucose challenge test for screening of gestational diabetes mellitus.* J Obstet Gynaecol, 2013. **33**(5): p. 447-50.
22. Kempf, K., et al., *Screening for overt diabetes by oral glucose tolerance test: stratification by fasting blood glucose and patients' age improve practicability of guidelines in cardiological routine.* Int J Cardiol, 2011. **150**(2): p. 201-5.
23. van Leeuwen, M., et al., *Fasting capillary glucose as a screening test for gestational diabetes mellitus.* BJOG, 2007. **114**(3): p. 372; author reply 373.
24. Rey, E., et al., *Fasting plasma glucose versus glucose challenge test: screening for gestational diabetes and cost effectiveness.* Clin Biochem, 2004. **37**(9): p. 780-4.
25. Kosus, N., et al., *Effect of number of abnormal oral glucose tolerance test (OGTT) values on birthweight in women with gestational diabetes.* Indian J Med Res, 2013. **137**(1): p. 95-101.
26. Hayashi, T., et al., *Patterns of insulin concentration during the OGTT predict the risk of type 2 diabetes in Japanese Americans.* Diabetes Care, 2013. **36**(5): p. 1229-35.
27. De Gaetano, A., et al., *Routine OGTT: a robust model including incretin effect for precise identification of insulin sensitivity and secretion in a single individual.* PLoS One, 2013. **8**(8): p. e70875.
28. Hagura, R., *[Oral glucose tolerance test (OGTT) for diagnosis of diabetes mellitus].* Nihon Rinsho, 2005. **63 Suppl 2**: p. 372-5.
29. Ito, C., et al., *Importance of OGTT for diagnosing diabetes mellitus based on prevalence and incidence of retinopathy.* Diabetes Res Clin Pract, 2000. **49**(2-3): p. 181-6.
30. Michaelis, D., et al., *[Clinically relevant problems of oGTT evaluation following the new classification criteria of diabetes mellitus and glucose tolerance disorders].* Z Arztl Fortbild (Jena), 1986. **80**(5): p. 209-15.
31. Vaddiraju, S., et al., *Design and fabrication of a high-performance electrochemical glucose sensor.* J Diabetes Sci Technol, 2011. **5**(5): p. 1044-51.
32. Vaddiraju, S., et al., *Enhanced glucose sensor linearity using poly(vinyl alcohol) hydrogels.* J Diabetes Sci Technol, 2009. **3**(4): p. 863-74.
33. Croce, R.A., Jr., et al., *A miniaturized transcutaneous system for continuous glucose monitoring.* Biomed Microdevices, 2013. **15**(1): p. 151-60.
34. Wang, Y., B. Gu, and D.J. Burgess, *Microspheres Prepared with PLGA Blends for Delivery of Dexamethasone for Implantable Medical Devices.* Pharm Res, 2013.
35. Bhardwaj, U., et al., *PLGA/PVA hydrogel composites for long-term inflammation control following s.c. implantation.* Int J Pharm, 2010. **384**(1-2): p. 78-86.
36. Bhardwaj, U., et al., *Controlling acute inflammation with fast releasing dexamethasone-PLGA microsphere/pva hydrogel composites for implantable devices.* J Diabetes Sci Technol, 2007. **1**(1): p. 8-17.
37. Hickey, T., et al., *Dexamethasone/PLGA microspheres for continuous delivery of an anti-inflammatory drug for implantable medical devices.* Biomaterials, 2002. **23**(7): p. 1649-56.
38. Hickey, T., et al., *In vivo evaluation of a dexamethasone/PLGA microsphere system designed to suppress the inflammatory tissue response to implantable medical devices.* J Biomed Mater Res, 2002. **61**(2): p. 180-7.

39. Patil, S.D., F. Papadmitrakopoulos, and D.J. Burgess, *Concurrent delivery of dexamethasone and VEGF for localized inflammation control and angiogenesis.* J Control Release, 2007. **117**(1): p. 68-79.

Chapter 2

Prevention of Foreign Body Reaction in a Pre-Clinical Large Animal Model

Abstract

In this work, the foreign body reaction (FBR) to small subcutaneous implants was compared between small (rodent) and large (swine) animal species for the first time. Dexamethasone-releasing poly(lactic-co-glycolic acid) microspheres/polyvinyl alcohol hydrogel composite coatings were adapted to prevent FBR to small, subcutaneous implants in a large animal model (Goettingen minipigs). The implants consisted of small silicon chips (used to mimic small medical devices) that were coated with the composite formulations. The stages of the FBR were compared with previous studies in rats (that used the same-sized implants); the onset and severity of chronic inflammation (collagen deposition) was identified as a key difference between the two species. In the absence of inflammation control, fibrosis was observed from day 7 post-implantation in minipigs, whereas in rats this did not occur until day 14. This is significant as swine skin is the most commonly used model for preclinical testing of dermal formulations. It was determined that for long-term prevention of the FBR (longer than 24 hours), a lag phase in dexamethasone release between days 1 and 10 did not affect the anti-FBR properties of the implant in rats. However, continuous release of dexamethasone, with no lag phase, was necessary to prevent inflammation in minipigs (effective dexamethasone dose was 100 μg delivered immediately after implantation and 10 μg/day delivered continuously thereafter). This study offers significant insight into the translation of anti-FBR strategies across species, and showcases the importance of tailoring the controlled release kinetics of the formulation to the host response.

2.1. Introduction

Implantable biomaterials such as biosensors are recognized by the immune system as foreign; this leads to a cascade of events collectively known as the foreign body reaction (FBR)[1, 2]. The FBR consists of two main phases: an acute phase, characterized by the infiltration of inflammatory cells, mainly neutrophils, and a chronic phase, characterized by the presence of active fibroblasts (cells that deposit collagen fibers around the implant)[1, 3-5]. The collagen fibers will ultimately encapsulate the foreign body in a dense, fibrous collagen layer (fibrosis).

The FBR has been the focus of many research studies over the past decades. Most of the early work in this area was related to organ rejection prevention[6-8]. In recent years, the emergence of implantable medical devices has led to the FBR being investigated to extend device lifetime[9-12]. In the case of subcutaneously implanted devices, their size, shape, mechanical properties, type of biomaterial, implantation duration and even method of implantation can yield a different response. The FBR can be minimized by using materials with mechanical properties similar to those of the surrounding tissue[13-15], by incorporating hydrophilic coatings that prevent protein adsorption (biofouling)[16-20] and by using biocompatible materials that do not produce toxic or irritating by-products upon degradation[21-24]. However, these approaches only minimize the FBR but do not eliminate it altogether. The only method that has been shown to completely prevent the FBR is the use of local delivery of anti-inflammatory agents which prevent infiltration and further attraction of inflammatory cells[25-32]. Systemic administration of anti-inflammatory agents and immuno-suppressants is regularly used to prevent organ rejection[33-41] but it is not a desirable approach for medical devices and implantable biomaterials due to the high risk-to-benefit ratio.

Dexamethasone, a synthetic glucocorticoid, is the most commonly used anti-inflammatory agent to prevent FBR[26, 27, 29, 31]. Due to its potency, only small amounts of dexamethasone are required; this is essential for small implants where space is limited. Implant coatings designed to suppress the FBR for implantable glucose biosensors have been previously reported and their efficacy has been tested in several rat models (normal, diabetic, and obese) for one and three month implantation durations[9, 11, 28, 42-46]. Dexamethasone was delivered throughout the implantation period by incorporation in poly(lactic-co-glycolic acid) (PLGA) microspheres that were embedded in a polyvinyl alcohol (PVA) hydrogel coating. While studying the efficacy of these coatings in small animals is necessary as proof-of-concept, it is accepted that studies in larger animals are required in order to extrapolate the results to design the first-in-human clinical trials. The Goettingen minipig, a breed of miniature swine, is a common animal model for dermal studies due to the similarities between human and swine skin[47-50]. The objective of the present work was to study the FBR to miniaturized implantable biomaterials in the Goettingen minipig, identify key parameters that will determine anti-FBR dosing regimens of dexamethasone, and apply the findings for long-term prevention of the FBR. To achieve this, PLGA microsphere/PVA hydrogel composites that release dexamethasone in various amounts and rates (as determined in previously published work from our group[51]) were prepared. The composites were used to coat silicon chips, mimicking an implantable biosensor, and were implanted in the subcutaneous tissue of Goettingen minipigs. The local tissue reaction to the implants was determined histologically at multiple time points after implantation.

2.2. Materials and Methods

2.2.1. Materials

Dexamethasone was purchased from Cayman Chemical Company (Ann Arbor, MI). High-molecular weight poly(vinyl alcohol) (HMW-PVA, MW 30–70 kDa), was purchased from Polysciences, Inc. (Warrington, PA) and low-molecular weight PVA (LMW-PVA, 99 % hydrolyzed, MW 133 kDa) was purchased from Sigma-Aldrich (St. Louis, MO). PLGA Resomer® RG503H (inherent viscosity 0.32–0.44 dl/g) was a gift from Boehringer-Ingelheim and PLGA DLG2A (inherent viscosity 0.15–0.25 dl/g), was a gift from SurModics Pharmaceuticals (Birmingham, AL). Methylene chloride and dimethyl sulfoxide (DMSO, ACS grade) were purchased from Fisher Scientific (Pittsburghm, PA).

2.2.2. PLGA microsphere preparation.

Dexamethasone-loaded PLGA microspheres were prepared as previously described9. Briefly, 2 g of PLGA were dissolved in 8 ml methylene chloride (DCM). 200 mg of crystalline dexamethasone were added to the polymer solution and the mixture was homogenized at 10,000 rpm for 2.5 min using a T 25 digital ULTRA-TURRAX® homogenizer (IKA® Works, Inc.) to obtain a homogenous suspension. The suspension was subsequently transferred to 40 ml of 1% w/v LMW-PVA aqueous solution and homogenized for 1 min at 10,000 rpm to obtain a solid-oil-water emulsion. The emulsion was transferred to 500 ml of 0.1% w/v LMW-PVA aqueous solution and stirred at 600 rpm under vacuum for 3 hours to remove the DCM. The hardened microspheres were purified *via* three centrifugation cycles at 3,500 rpm for 2 min each, freeze dried and stored at 4 ^{o}C until further use. Blank microspheres were prepared in the same way without the addition of dexamethasone. PLGA polymers of two molecular weights were used in different preparations: 25,000 g/mol (50:50 Resomer 503H) and 12,000 g/mol (50:50 DLG 2A).

2.2.3. Preparation of implants

Implants were of cylindrical shape and consisted of a rectangular silicon chip core (5x0.5x0.5 mm) coated with PVA hydrogel embedded with PLGA microspheres (7-11 mm length, 1.5 mm diameter when hydrated). To coat the silicon chips, 75 or 150 mg of microspheres were suspended in 1 ml of 5% w/v HMW-PVA aqueous solution. The mixture was vortexed and placed in a sonicated bath for 10 seconds to achieve good microsphere distribution and break any aggregates. The PVA hydrogel was formed after physical crosslinking of the HMW-PVA *via* three freeze thaw cycles. First, the suspension was subjected to one freeze-thaw cycle (2 h at -20 ^{o}C and 1 h at ambient temperature). After the first cycle, the partially thickened suspension was fed in a two-piece grooved mold (grooves of 1.5 mm in diameter). The silicon chips were sandwiched between the two mold pieces that were then subjected to two more freeze-thaw cycles to complete the PVA crosslinking and form a self-supporting hydrogel around the chips. Each mold was used to coat 30 silicon chips of approximately 2 mg weight. Please note that low-molecular weight PVA was used as a surfactant to improve emulsion stability during the microsphere preparation process, while high-molecular weight PVA was used to form a hydrogel. Hydrogel strips containing the silicon chips were air-dried and cut at 7, 9 or 11 mm length implants. The implants were placed in 16 gauge needles and stored at 4 ^{o}C until further use. Different implant formulations were labeled as shown in Table 2.1.

2.2.4. PLGA microsphere characterization

Particle size: An Accusizer 780 (Particle Sizing Systems) was used to measure the particle size of the PLGA microspheres. 3-5 mg of dried microspheres were suspended in 1 ml of 0.1% w/v LMW-PVA solution, bath-sonicated for 10 s and analyzed for volume-based average size.

Dexamethasone loading: 5 mg of dried microspheres or composites were dissolved in 1 ml DMSO and then diluted 10 times in phosphate buffered saline (PBS) pH 7.4. Dexamethasone

concentration was determined *via* RP-HPLC (PerkinElmer, Inc.). Mobile phase: acetonitrile/water/phosphoric acid (30/70/0.5%, v/v/v); column: Zorbax® C18 (4.6 mm×15 cm); detection wavelength: 240 nm; flow rate: 1 ml/min.

2.2.5. *In vivo* pharmacodynamics study

Seven young, female Goettingen minipigs were used as a large animal model to study the inhibition of the FBR to subcutaneous implants. Minipigs were studied in iterations of 2 or 3 animals. The number of animals that were utilized for each formulation is indicated in the figure legends. Each study lasted for 30 days. The implants that were tested are shown in Table 2.1. They were implanted at the back of the animals on days 0, 9, 16, 23, 27, and 29. All implants were spaced at least 5 cm apart to ensure no interference. The area right above the spinal cord was not implanted. The animals were sacrificed on day 30 and the implants with surrounding subcutaneous tissue were harvested and stored in 10% buffered formalin solution (Sigma-Aldrich Co. LLC.). This resulted in implants being excised on days 1, 3, 7, 14, 21, and 30 post-implantation. All time points were ± 3 days to allow for unforeseeable delays. The extracted implants that prevented the FBR were analyzed for the remaining dexamethasone content. All animal studies were reviewed and approved by the University of Connecticut's Institutional Animal Care and Use Committee (IACUC) prior to the beginning of the experiments.

2.2.6. Histological evaluation

Fixed tissues were processed, embedded in paraffin and sectioned in 20 μm films at the University of Connecticut's Pathobiology Department. Tissue sections were stained with Hematoxylin & Eosin (H&E) and the presence and progress of the FBR was evaluated by observation under a light microscope. Normal connective tissue appears pink, adipose tissue white,

deposited collagen fibers light pink, and inflammatory cells purple. Digital images representative of the tissue reaction around the implants are presented here.

2.3. Results

2.3.1. Microsphere characterization

Physical properties of the microspheres were measured to confirm that the formulations were consistent with the previous work[51]. The particle size and drug loading of the microspheres are shown in Table 2.2. Please note that due to the low solubility of dexamethasone in water and some polymer loss during microsphere preparation, the dexamethasone loading exceeded the theoretical (10% by weight).

2.3.2. FBR to implants with no dexamethasone

Implants coated with blank (no dexamethasone) microspheres embedded in PVA hydrogel were used to study the FBR in Goettingen minipigs. Tissue sections excised at 3, 7, 14, 21 and 30 days after implantation give a representation of the progress of the FBR (Figure 2.1).

The FBR consisted of the typical acute phase observed on day 3 (indicated by the presence of purple-stained inflammatory cells around the implant), and the chronic phase with fibrous encapsulation clearly visible from day 14 onwards (observed as a light pink band with collagen fibers oriented around the implant). Collagen deposition around the implant can be clearly seen on day 7 prior to fibrous encapsulation (Figure 2.2).

2.3.3. Effect of total dexamethasone dose

Implants coated with dexamethasone-loaded composites were used to determine whether the formulation that was effective in normal, diabetic and obese rats can be used in large animals. Implant *R* was the reference formulation which had the same composition as that which was

effective in all rat models9. Implants with higher dexamethasone doses were also tested in order to optimize the dexamethasone dosing. Two strategies to increase the total dexamethasone per implant were employed: *a)* doubling the microsphere density in the coating to 150 mg per 1 ml of PVA hydrogel (the maximum microsphere content that allows enough glucose permeability through the implant as determined in previous studies, unpublished data by Burgess *et. al.*); and *b)* increasing the implant length from 7 to 11 mm. All implant preparations are detailed in Table 2.1.

As shown in Figure 2.3, the implants with the higher dexamethasone doses (implants *R150* and *R11*) completely suppressed the acute inflammation as no cell infiltration was observed on day 3 post-implantation. Implants *R* and *R9* with lower dexamethasone doses, including the reference implant, did not completely prevent the acute inflammatory phase but did reduce it significantly compared to the control. However, none of the implants prevented the chronic phase of the FBR, and collagen deposition is observed from day 7 in all cases, with the fibrous capsule being observed from day 14. The implants with the higher dexamethasone doses (implants *R150* and *R11*) showed relatively less dense fibrous capsules compared to the control implants, however, this is not satisfactory for the purpose of long-term prevention of FBR to prolong the functionality of implantable biomaterials.

2.3.4. Effect of PLGA molecular weight

Implants made with PLGA microspheres of lower molecular weight were tested. These microspheres release dexamethasone continuously for two weeks, with no lag phase, as previously reported51. A formulation with lower molecular weight PLGA microspheres loaded in PVA hydrogels with the maximum amount (150 mg per 1 ml hydrogel) was tested (implant *R2W*). As shown in Figure 2.4 this formulation prevented acute inflammation (no inflammatory cell

accumulation, pane A in Figure 2.4) as well as chronic inflammation (no fibrous encapsulation, panel D in Figure 2.4) up to day 11. Minimal collagen deposition was observed on day 14 when dexamethasone was depleted. Implants extracted 1 and 14 days after implantation were analyzed for dexamethasone content. It was determined that after 24 hours, 61.56 ± 5.72 % of dexamethasone remained in the implant (*i.e.* 35.16 ± 5.72 % released during the burst phase) while 7.77 ± 1.82 % remained in the implant at the end of 14 days (*i.e.* 92.81 ± 1.82 % released). Accordingly, the effective dexamethasone dose was calculated based on 40% of the total dexamethasone released during the first 24 hours and the rest continuously released throughout the implantation period (approximately 100 μg released the first day and 10 μg/day throughout the remainder of the implantation period).

2.4. Discussion

Local delivery of dexamethasone, an anti-inflammatory agent, has been successfully used to counter the FBR to subcutaneously-implanted biomaterials in normal, obese and diabetic rats. In order to translate this technology to the clinic, it was decided to bridge the gap between rats and humans by using a large animal model, Goettingen minipigs. The progress and prevention of the FBR was studied, with the intention to directly compare the finding with corresponding investigations in rats. Direct comparison was made possible by starting with implants with the same characteristics as the ones that were previously tested in rats (size, shape, mechanical properties, materials, anti-inflammatory drug)[9.] Our results reveal critical factors that need to be taken into consideration when extrapolating this type of data across different species.

It was found that while the events leading to fibrotic encapsulation are similar between minipigs and rats, their timing differs significantly. In rats, fibroblast recruitment and activation starts 14 days after implantation[42], while in minipigs active fibroblasts and collagen deposition can

be observed from day 7. This is shown in Figure 2.1 panel c and in Figure 2.2 where a dense collagen network surrounds the implant. This network will later on contract to form the fibrotic membrane isolating the implant. In the corresponding studies in rats, no dense collagen network was observed on day 7 after implantation. Instead, loose connective tissue similar to subcutaneous tissue under normal conditions was observed. The difference in the onset of fibrosis between rats and minipigs is of great importance as it indicates a difference in the severity of the chronic inflammation between the two species and consequently the amount of drug necessary to counter it.

In transition from small to large animals during preclinical testing of drug-releasing formulations, dose is usually scaled up according to body weight with corrections based on empirical formulas. In the case of locally-acting implants, however, dose scale-up is not necessary as no systemic effect is desired. In order to prevent the FBR to devices implanted in the subcutaneous tissue, a minimum level of drug has to be maintained in the local environment throughout the implantation period. This level may vary from species to species due to differences in drug clearance from the subcutaneous tissue, drug diffusion rates through the tissue, drug metabolism and the presence of cells.

Implants made of PLGA microspheres of the same molecular weight as the ones tested in rats and same total dexamethasone loading were used as reference formulations. These implants did not prevent the FBR and the tissue surrounding them was similar to that around the control implants. As evidenced by the absence of inflammatory cell accumulation in Figure 2.3, higher dexamethasone doses prevented the acute phase of the FBR. The higher dexamethasone doses were achieved by either increasing the microsphere density in the biocompatible coating or increasing the total length of the implants. However, increasing the dexamethasone dose was

limited due to the small size of the implants. The maximum amount of dexamethasone per implant that was achieved was 0.22 mg. This amount was not enough to prevent fibrous encapsulation of the implants.

Based on the *in vitro* dissolution testing of these implants[51], 40% of the drug is released within the first 24 hours and the remaining amount is released continuously starting from about day 10 post-implantation. This leaves a nine-day period with little-to-no dexamethasone release in the tissue (lag phase). The lag phase did not interfere with the anti-FBR effect of the implants in rats. Based on the observations on the earlier timing of fibrosis onset in minipigs compared to rats, it was hypothesized that eliminating this lag phase might prevent FBR. This hypothesis was tested and confirmed using PLGA microspheres of a lower molecular weight. Implants made with these microspheres release dexamethasone continuously for about 14 days with no lag phase[51]. Once implanted in the minipigs, the implants prevented the FBR until day 11 and early collagen deposition is observed on day 14. This is likely due to the dexamethasone depletion that occurs around that time.

Based on the results discussed above, the dexamethasone dose that is effective to counter the FBR in Goettingen minipigs is ~100 μg released during the first day (to counter the acute inflammation cause by tissue trauma) and about 10 μg/day released continuously throughout the implantation period (to prevent fibroblast activation and collagen deposition). This was confirmed following analysis of the amount of dexamethasone remaining in exctracted implants at 24 hours and 14 days. This dosing regimen applies to subcutaneously-implanted materials of small size (around 7x1.5 mm when hydrated). It has been previously shown that the size of the implant affects the severity of the FBR in rats, so dose adjustment will likely be necessary for implants of different

sizes. The release kinetics of dexamethasone, however, will have to remain the same, *i.e.* a burst release followed by a continuous, zero-order release throughout the implantation period.

The size of our implants was chosen to reflect the trend of miniaturization of implantable medical devices. The extent of the anti-inflammatory drug dose limitation varies from implant to implant and it depends on implant size, desired coating thickness, desired coating permeability to various tissue molecules, and the type of controlled release vesicle used to deliver the drug. In order to extend the anti-FBR effect of the biomaterials beyond the two-week period achieved here, the drug-carrier technology (in this case the PLGA microspheres) has to be optimized or replaced in order to maximize the drug loading efficiency and accommodate high dexamethasone doses in such small samples.

2.5. Conclusions

In the present work, the FBR to subcutaneous implants was compared between a small and large animal model for the first time. The onset and severity of fibrosis was identified as a key difference with minipigs, demonstrating earlier onset and more severe chronic inflammation compared to rats. It was determined that the dexamethasone release from the implant coatings must be tailored to the species-specific stages of the FBR. In order to counter the more severe chronic inflammation observed in minipigs compared to rats, dexamethasone release must be continuous, with no lag phase. The effective dexamethasone dosing regime was 100 μg during the first day and 10 μg/day thereafter; this regime is applicable to implants of similar size (7 x 0.15 mm) and can be extrapolated to longer implantation periods in minipigs. Lastly, these findings can facilitate the dose calculations in the first-in-human studies as porcine skin is the optimal model for dermal formulations.

2.6. References

1. Morais JM, Papadimitrakopoulos F, Burgess DJ. Biomaterials/tissue interactions: possible solutions to overcome foreign body response. The AAPS journal. 2010;12:188-96.
2. Kenneth Ward W. A review of the foreign-body response to subcutaneously-implanted devices: the role of macrophages and cytokines in biofouling and fibrosis. Journal of diabetes science and technology. 2008;2:768-77.
3. Thiele A, Bilkenroth U, Bloching M, Knipping S. Foreign body reaction to materials implanted as biocompatible for internal fixation. Hno. 2008;56:545-8.
4. Wallace SA, Brown KL. Foreign body reaction to sutures and other materials. Texas state journal of medicine. 1948;44:463-6.
5. Swingle KF, Shideman FE. Phases of the inflammatory response to subcutaneous implantation of a cotton pellet and their modification by certain anti-inflammatory agents. The Journal of pharmacology and experimental therapeutics. 1972;183:226-34.
6. Ferrell LD, Lee R, Brixko C, Bass NM, Lake JR, Roberts JP, et al. Hepatic granulomas following liver transplantation. Clinicopathologic features in 42 patients. Transplantation. 1995;60:926-33.
7. Kinoshita Y, Kirigakubo M, Kobayashi M, Tabata T, Shimura K, Ikada Y. Study on the efficacy of biodegradable poly(L-lactide) mesh for supporting transplanted particulate cancellous bone and marrow: experiment involving subcutaneous implantation in dogs. Biomaterials. 1993;14:729-36.
8. Congdon CC. Bone marrow transplantation. Science. 1971;171:1116-24.
9. Wang Y, Papadimitrakopoulos F, Burgess DJ. Polymeric "smart" coatings to prevent foreign body response to implantable biosensors. Journal of controlled release : official journal of the Controlled Release Society. 2013;169:341-7.
10. Bhardwaj U, Papadimitrakopoulos F, Burgess DJ. A review of the development of a vehicle for localized and controlled drug delivery for implantable biosensors. Journal of diabetes science and technology. 2008;2:1016-29.
11. Bhardwaj U, Sura R, Papadimitrakopoulos F, Burgess DJ. Controlling acute inflammation with fast releasing dexamethasone-PLGA microsphere/pva hydrogel composites for implantable devices. Journal of diabetes science and technology. 2007;1:8-17.
12. Vaddiraju S, Burgess DJ, Tomazos I, Jain FC, Papadimitrakopoulos F. Technologies for continuous glucose monitoring: current problems and future promises. Journal of diabetes science and technology. 2010;4:1540-62.
13. Lips PA, van Luyn MJ, Chiellini F, Brouwer LA, Velthoen IW, Dijkstra PJ, et al. Biocompatibility and degradation of aliphatic segmented poly(ester amide)s: in vitro and in vivo evaluation. Journal of biomedical materials research Part A. 2006;76:699-710.
14. Liu Y, Zheng Shu X, Prestwich GD. Biocompatibility and stability of disulfide-crosslinked hyaluronan films. Biomaterials. 2005;26:4737-46.
15. Pol BJ, van Wachem PB, van Luyn MJ, van der Does L, Bantjes A. In vivo testing of crosslinked polyethers. I. Tissue reactions and biodegradation. Journal of biomedical materials research. 1996;32:307-20.
16. Zhang H, Bian C, Jackson JK, Khademolhosseini F, Burt HM, Chiao M. Fabrication of robust hydrogel coatings on polydimethylsiloxane substrates using micropillar anchor structures with chemical surface modification. ACS applied materials & interfaces. 2014;6:9126-33.
17. Lin P, Lin CW, Mansour R, Gu F. Improving biocompatibility by surface modification techniques on implantable bioelectronics. Biosensors & bioelectronics. 2013;47:451-60.

18. Li Y, Liu CM, Yang JY, Gao YH, Li XS, Que GH, et al. Anti-biofouling properties of amphiphilic phosphorylcholine polymer films. Colloids and surfaces B, Biointerfaces. 2011;85:125-30.
19. Scardino AJ, Zhang H, Cookson DJ, Lamb RN, de Nys R. The role of nano-roughness in antifouling. Biofouling. 2009;25:757-67.
20. Dahlstrom M, Jonsson PR, Lausmaa J, Arnebrant T, Sjogren M, Holmberg K, et al. Impact of polymer surface affinity of novel antifouling agents. Biotechnology and bioengineering. 2004;86:1-8.
21. Maiborodin IV, Kuznetsova IV, Beregovoi EA, Shevela AI, Barannik MI, Maiborodina VI, et al. Reaction of rat tissues to implantation of lactic acid-based biodegradable polymer. Bulletin of experimental biology and medicine. 2014;156:874-9.
22. Kuznetsova IV, Maiborodin IV, Shevela AI, Barannik MI, Manaev AA, Brombin AI, et al. Local tissue reaction to implantation of biodegradable suture materials. Bulletin of experimental biology and medicine. 2014;157:390-4.
23. Hernandez KA, Hooper RC, Boyko T, Golas AR, van Harten M, Wu DQ, et al. Reduction of suture associated inflammation after 28 days using novel biocompatible pseudoprotein poly(ester amide) biomaterials. Journal of biomedical materials research Part B, Applied biomaterials. 2014.
24. Ronkko S, Kaarniranta K, Kalesnykas G, Uusitalo H. Biocompatibility of different poly(lactide-coglycolide) polymers implanted into the subconjunctival space in rats. Ophthalmic research. 2011;46:55-65.
25. Khurana RN, Appa SN, McCannel CA, Elman MJ, Wittenberg SE, Parks DJ, et al. Dexamethasone implant anterior chamber migration: risk factors, complications, and management strategies. Ophthalmology. 2014;121:67-71.
26. Liu X, De Scheerder I, Desmet W. Dexamethasone-eluting stent: an anti-inflammatory approach to inhibit coronary restenosis. Expert review of cardiovascular therapy. 2004;2:653-60.
27. Hickey T, Kreutzer D, Burgess DJ, Moussy F. Dexamethasone/PLGA microspheres for continuous delivery of an anti-inflammatory drug for implantable medical devices. Biomaterials. 2002;23:1649-56.
28. Hickey T, Kreutzer D, Burgess DJ, Moussy F. In vivo evaluation of a dexamethasone/PLGA microsphere system designed to suppress the inflammatory tissue response to implantable medical devices. Journal of biomedical materials research. 2002;61:180-7.
29. Frucht-Pery J, Siganos CS, Solomon A, Shvartzenberg T, Richard C, Trinquand C. Topical indomethacin solution versus dexamethasone solution for treatment of inflamed pterygium and pinguecula: a prospective randomized clinical study. American journal of ophthalmology. 1999;127:148-52.
30. Radovsky AS, Van Vleet JF. Effects of dexamethasone elution on tissue reaction around stimulating electrodes of endocardial pacing leads in dogs. American heart journal. 1989;117:1288-98.
31. Rosenthal AR, Appleton B, Zimmerman R, Hopkins JL. Intraocular copper foreign bodies. Use of dexamethasone to suppress inflammation. Archives of ophthalmology. 1976;94:1571-6.
32. Sasabe T. Studies on experimental pathology using dexamethasone with reference to its influence on the living body. Zasshi Tokyo Ika Daigaku. 1967;25:937-74.

33. Khatri P, Roedder S, Kimura N, De Vusser K, Morgan AA, Gong Y, et al. A common rejection module (CRM) for acute rejection across multiple organs identifies novel therapeutics for organ transplantation. The Journal of experimental medicine. 2013;210:2205-21.
34. Okamoto T, Okamoto S, Fujimoto Y, Tabata Y, Uemoto S. Suppression of acute rejection by administration of prostaglandin E2 receptor subtype 4 agonist in rat organ transplantation models. The Journal of surgical research. 2013;183:852-9.
35. Zhang H, Chen L, Gu G, Guo Z, Gong F, Wu S, et al. Clinical observation and nursing care on the prevention of abdominal organ cluster transplantation rejection. Journal of clinical nursing. 2013;22:1599-603.
36. Alvarado LG. The problem of rejection in organ transplants. Revista brasileira de medicina. 1969;26:427-8.
37. Corman JL, Kashiwagi N, Porter KA, Andres G, Iwatsuki S, Putnam CW, et al. Unsuccessful attempts to control hyperacute rejection of human renal homografts with F(ab') 2 and citrate organ pretreatment. Transplantation. 1973;16:60-3.
38. Dalton RG. Rejection: the major problem of organ transplantation in man and animals. The Veterinary record. 1974;94:333-6.
39. Stella F, Alfani D, Stella C, Battistelli S, Troccoli R, Cortesini R. Differential diagnosis of rejection and cyclosporin nephrotoxicity in organ transplantation using exfoliative urinary cytology. Quaderni Sclavo di diagnostica clinica e di laboratorio. 1985;21:330-40.
40. Venkataramanan R, Ptachcinski RJ, Burckart GJ, Yang S, Starzl TE. Extraction ratio of cyclosporine in a liver transplant patient with organ rejection. Journal of pharmaceutical sciences. 1985;74:901-2.
41. Bach JF. Renewal of organ transplantation: towards the control of rejection. La Revue du praticien. 1986;36:1615-9.
42. Patil SD, Papadimitrakopoulos F, Burgess DJ. Dexamethasone-loaded poly(lactic-co-glycolic) acid microspheres/poly(vinyl alcohol) hydrogel composite coatings for inflammation control. Diabetes technology & therapeutics. 2004;6:887-97.
43. Patil SD, Papadmitrakopoulos F, Burgess DJ. Concurrent delivery of dexamethasone and VEGF for localized inflammation control and angiogenesis. Journal of controlled release : official journal of the Controlled Release Society. 2007;117:68-79.
44. Zolnik BS, Burgess DJ. Evaluation of in vivo-in vitro release of dexamethasone from PLGA microspheres. Journal of controlled release : official journal of the Controlled Release Society. 2008;127:137-45.
45. Bhardwaj U, Sura R, Papadimitrakopoulos F, Burgess DJ. PLGA/PVA hydrogel composites for long-term inflammation control following s.c. implantation. International journal of pharmaceutics. 2010;384:78-86.
46. Wang Y, Vaddiraju S, Qiang L, Xu X, Papadimitrakopoulos F, Burgess DJ. Effect of dexamethasone-loaded poly(lactic-co-glycolic acid) microsphere/poly(vinyl alcohol) hydrogel composite coatings on the basic characteristics of implantable glucose sensors. Journal of diabetes science and technology. 2012;6:1445-53.
47. Ploemen IH, Hirschberg HJ, Kraan H, Zeltner A, van Kuijk S, Lankveld DP, et al. Minipigs as an animal model for dermal vaccine delivery. Comparative medicine. 2014;64:50-4.
48. Dame MK, Spahlinger DM, DaSilva M, Perone P, Dunstan R, Varani J. Establishment and characteristics of Gottingen minipig skin in organ culture and monolayer cell culture:

relevance to drug safety testing. In vitro cellular & developmental biology Animal. 2008;44:245-52.
49. Mahl JA, Vogel BE, Court M, Kolopp M, Roman D, Nogues V. The minipig in dermatotoxicology: methods and challenges. Experimental and toxicologic pathology : official journal of the Gesellschaft fur Toxikologische Pathologie. 2006;57:341-5.
50. Dincer Z, Jones S, Haworth R. Preclinical safety assessment of a DNA vaccine using particle-mediated epidermal delivery in domestic pig, minipig and mouse. Experimental and toxicologic pathology : official journal of the Gesellschaft fur Toxikologische Pathologie. 2006;57:351-7.
51. 51 Shen J, Burgess DJ. Accelerated in vitro release testing of implantable PLGA microsphere/PVA hydrogel composite coatings. International journal of pharmaceutics. 2012;422:341-8.

Chapter 3

Development of Dexamethasone-Loaded PLGA Microspheres for Long-Term Prevention of the Foreign Body Reaction in Gottingen Minipigs

Abstract

An important strategy currently used to prevent the foreign body reaction (FBR) to subcutaneous implants in animal models is the constant release of dexamethasone in the tissue surrounding the implant. There have been few studies in large animal models including: 1) a bulky osmotic pump system that delivers dexamethasone over a one-month period; and 2) a poly(lactic-co-glycolic acid) (PLGA) microsphere/polyvinyl alcohol (PVA) hydrogel composite coating for miniaturized implants that locally delivers dexamethasone for a two-week period in minipigs. A long-term strategy to prevent FBR to subcutaneous implants in a large animal model is necessary. In this work, a PLGA microsphere/PVA hydrogel composite coating for the one-month prevention of the FBR in Gottingen minipigs was developed. This coating is suitable for miniaturized implantable devices (of a few mm length), such as biosensors, that require constant communication with the local microenvironment to function. The microspheres were prepared *via* dexamethasone/polymer co-precipitation which resulted homogeneous distribution of dexamethasone in the microsphere matrix which in turn gave rise to increased drug loading, low burst release, and minimal lag phase. The *in vivo* functionality of the composite coatings was evaluated *via* histological examination of explanted tissue samples from the area surrounding the implants.

Keywords: PLGA microspheres; dexamethasone; foreign body reaction; swine; co-precipitation.

3.1. Introduction

Once implanted, biomaterials face the host tissue's response (foreign body reaction, FBR) which often interferes with their intended action[1-8]. The final result of the FBR is isolation of the implant from the surrounding tissue *via* fibrous encapsulation[9-11]. This can inhibit drug transport in the case of drug-delivering biomaterials, prevents healing in the case of tissue engineering scaffolds, and stops analyte diffusion in the case of implantable biosensors. The effect of, as well as the prevention of FBR for various types of biomaterials has been studied using different animal models[11-14].

The FBR consists of a cascade of events that includes, among others, inflammatory cell recruitment, collagen deposition, and formation of an avascular fibrotic capsule around the foreign body. Most of these steps are preserved across different species, however, some differences exist. It has been reported that diabetic rats lack the high levels of mast cells that are observed in normal rat subcutaneous tissue during the FBR[15]. The function of mast cells is to exacerbate acute inflammation and as a result diabetic rats show a less severe response in the days immediately following implantation. Other parts of the FBR have been compared between different species, such as nitric oxide production from human, mouse and rat macrophages[16] and the presence of basophilic granules in humans and pigs[17, 18].

Our group has previously developed poly(lactic-co-glycolic acid) (PLGA) microsphere/polyvinyl alcohol (PVA) hydrogel-based composites capable of preventing the FBR to subcutaneously-implanted materials[15, 19-24]. This is achieved *via* delivery of dexamethasone, a synthetic corticosteroid with potent anti-inflammatory properties. The dexamethasone dose and release kinetics have been optimized for up to a three-month implantation period[19] in rat models (normal, type 1 diabetic, obese[15]) as well as in a large animal model (Gottingen minipigs) for a

two-week implantation period. Ward *et al.* have studied the anti-inflammatory effect of subcutaneously delivered dexamethasone for one month in minipigs. However, they delivered large amounts of dexamethasone (ranging from 3 to 42 mg/implant or 0.05 to 0.7 mg/Kg body weight). Such large amounts of dexamethasone are not necessary for local prevention of FBR, can cause systemic effects, and cannot be incorporated around miniaturized implants (for example biosensors of a few millimeters in length). Accordingly, a method to deliver small amounts (less than one mg) of dexamethasone effectively to prevent FBR in a large animal model is necessary.

It was previously determined that: *a)* high dexamethasone loading in PLGA microspheres is necessary to provide sufficient drug to last for a one-month implantation period in minipigs; and *b)* a lag phase in the dexamethasone release profile is detrimental in preventing FBR in minipigs. Accordingly, in the present work a new PLGA microsphere formulation with high drug loading efficiency and no lag phase was developed. The new PLGA formulation was prepared *via* dexamethasone-PLGA co-precipitation rather than dexamethasone crystal dispersion in the PLGA matrix and its anti-FBR efficacy was tested in Gottingen minipigs for a one-month implantation period.

3.2. Materials and Methods

3.2.1. Materials

Dexamethasone was purchased from Cayman Chemical Company (Ann Arbor, MI). High-molecular weight poly(vinyl alcohol) (HMW-PVA, MW 30–70 kDa), was purchased from Polysciences, Inc. (Warrington, PA) and low-molecular weight PVA (LMW-PVA, 99 % hydrolyzed, MW 133 kDa) was purchased from Sigma-Aldrich (St. Louis, MO). PLGA Resomer® RG503H (inherent viscosity 0.32–0.44 dl/g) was a gift from Boehringer-Ingelheim and PLGA DLG2A (inherent viscosity 0.15–0.25 dl/g), was a gift from SurModics Pharmaceuticals

(Birmingham, AL). Methylene chloride and dimethyl sulfoxide (DMSO, ACS grade) were purchased from Fisher Scientific (Pittsburghm, PA).

3.2.2. Microsphere preparation

50 mg of dexamethasone were dissolved in a small amount of DMSO (0-200 μl). 200 mg PLGA were dissolved in 0.4 ml of DCM in a 50-ml Teflon vial. The dexamethasone solution was transferred into the polymer solution and vortexed at 3,000 rpm for 10 s to achieve a homogenous mixture. 10 or 20 ml of aqueous phase consisting of 1% w/v PVA in water and 0-30% v/v DMSO were added in the Teflon vial while vortexing at 3,000 rpm. The resulting emulsion was diluted in 380 ml Milli-Q water and was held at ambient temperature and pressure for 3 hours under stirring at 600 rpm. After 3 hours, stirring continued under vacuum for 30 min to remove any residual DMSO. The hardened microspheres were collected and any free PVA, DMSO and dexamethasone was removed *via* three centrifugation and washing (Milli-Q water) cycles at 3,500 rpm for 2 min each. The microspheres were subsequently freeze-dried and stored at 4 °C until further use.

3.2.3. Optimization of microsphere preparation method

The above method was optimized for dexamethasone solution volume, DMSO concentration in the aqueous phase, total volume of aqueous phase and dilution in Milli-Q water. The emulsions were monitored under a polarized light microscope (PLM) in order to pinpoint the position and timing of dexamethasone precipitation (inside *vs.* outside the emulsion droplets). The optimized formulation (slow homogeneous precipitation of dexamethasone within the emulsion droplets) was tested for burst release (dexamethasone released after 24 hours incubation at 37 °C, in 10 mM PBS) and was chosen for the remaining studies. A formulation where dexamethasone was not dissolved in DMSO but was suspended in the polymer solution was used as a negative control.

3.2.4. Characterization of PLGA microspheres

Particle size: An Accusizer 780 (Particle Sizing Systems) was used to measure the particle size of the PLGA microspheres. 3-5 mg of dried microspheres were suspended in 1 ml of 0.1% w/v PVA solution, bath-sonicated for 10 seconds (to break up any aggregates) and analyzed for volume-based average size.

Dexamethasone loading: 5 mg of dried microspheres or composites were dissolved in 1 ml DMSO and then diluted 10 times in phosphate buffered saline (PBS) pH 7.4. Dexamethasone concentration was determined *via* RP-HPLC (PerkinElmer, Inc.). Mobile phase: acetonitrile/water/phosphoric acid (30/70/0.5%, v/v/v); column: Zorbax® C18 (4.6 mm×15 cm); detection wavelength: 240 nm; flow rate: 1 ml/min.

3.2.5. Preparation of composite coatings

150 mg PLGA microspheres and 9 mg crystalline dexamethasone were added to 1 ml of PVA solution in water (5% w/v) and the mixture was bath-sonicated for 10 seconds to achieve a homogenous suspension. Please note that the coatings were spiked with crystalline dexamethasone to achieve approximately 100 μg dexamethasone release from each implant within the first 24 hours (due to the low burst release of the microspheres). This amount of burst release is necessary to prevent the first part of the FBR (acute inflammation) based on our previous studies. Small silicon chips (5x0.5x0.5 mm, used to mimic small implantable devices) were sandwiched between a two-piece grooved mold containing the microsphere/PVA suspension. The mold was subjected to three freeze-thaw cycles (2 h at -20 °C, 1 h at ambient temperature) to physically cross-link the PVA solution into a hydrogel that encloses the silicon chips. The coated chips were removed from the mold and cut into 7 mm length pieces, air-dried for 3 hours and stored at 4 °C until further use.

3.2.6. *In vitro* release testing of the composite coatings

Composites were placed in 10 ml of 10 mM PBS with 0.1% w/v sodium azide in amber vials. The vials were placed in a water-bath at 37 °C with stirring (100 rpm). The entire media volume was replaced periodically to ensure maintenance of sink conditions (total dexamethasone concentration in the media never exceeded 10% of the equilibrium solubility) and avoid the complication of dexamethasone degradation. The concentration of dexamethasone in the media was measured *via* HPLC as described above.

3.2.7. *In vivo* study

Six female Gottingen minipigs (4 months old) were used in this study. Three types of composites were studied: (A) coated chips with no dexamethasone, using blank PLGA microspheres as a negative control; (B) coated chips with optimized dexamethasone-loaded PLGA microspheres and crystalline dexamethasone; and (C) composites without silicon chips at the core with dexamethasone-loaded microspheres and crystalline dexamethasone. Group C was investigated in case the dexamethasone loaded in group B was insufficient to prevent FBR. Each minipig received three implants (subcutaneously injected at the back of the animals through a 16 G needle) on days 0, 9, 16, 23 and 27 and the animals were sacrificed on day 30. This resulted in samples being excised 3, 7, 14, 21 and 30 days after implantation. Excised composites with the surrounding tissue were fixed in 10% buffered formalin, and thin sections (20 μm) were stained using Hematoxylin & Eosin staining (H&E). H&E staining was chosen instead of Masson's trichrome (which stains collagen fibers blue). Due to the highly collagenous nature of swine subcutaneous tissue, slides that were stained with Masson's trichrome did not differentiate cytoplasm, interstitial fluid, and collagen deposition, since everything was stained blue. All animal

studies were reviewed and approved by the University of Connecticut's Institutional Animal Care and Use Committee.

3.2.8. Statistical analysis

All reported values are average values ± standard deviation based on three repetitions. The histological data were of a qualitative nature (presence or absence of inflammation) and representative images are shown.

3.3. Results

3.3.1. Optimization of microsphere preparation method

Rather than the typical method of suspending dexamethasone crystals in a PLGA solution, in this work the encapsulation of dexamethasone in PLGA microspheres was achieved by co-precipitation of dexamethasone and PLGA. The process was optimized in a pilot study where the precipitation of dexamethasone was visualized *via* PLM. Figure 3.1 shows two characteristic images: *a)* non-optimized process (no added DMSO in the external water phase which would have slowed down dexamethasone precipitation) where the dexamethasone crystals are observed outside the polymer phase (emulsion droplets); and *b)* optimized process where the dexamethasone crystals are located inside the polymer phase (emulsion droplets).

The optimized process is as mentioned in the Methods section 2.2, with the following specifications: 100 µl DMSO used to dissolve 50 mg of dexamethasone; 20 ml total volume of external aqueous phase; 30% v/v DMSO in the external aqueous phase; and primary emulsion dilution in 380 ml Milli-Q water. The optimized formulation was compared with the negative control formulation and representative images are shown in Figure 3.2.

3.3.2. Microsphere characterization

The optimized PLGA microspheres had a dexamethasone loading of 9 ± 0.13 % w/w, burst release (within 24 hours at 37 °C in 10 mM PBS pH 7.4) of 1.22 ± 0.17 %, and average size (based on volume distribution) of 36.36 ± 7.79 μm.

3.3.3. *In vitro* release

The release profile of dexamethasone from the composite coatings with the optimized PLGA microsphere formulation is shown in Figure 3.3. During the first 24 hours approximately 40 % of dexamethasone was released, which is as expected since the crystalline dexamethasone added to the composites accounted for 40 % of the total dexamethasone. A further 15 % was released during days 2 and 3. From day 4 onwards, sustained release of dexamethasone was observed, which exceeded 90 % of the total amount of drug in the composites by day 45. This portion of the release profile was approximately zero order with $R^2 = 0.9931$.

3.3.4. *In vivo* evaluation of the anti-FBR properties of the composite coatings

Figure 3.4 shows the progress of the FBR from day 3 to day 30 post-implantation for control implants (coated with blank composite coating, no dexamethasone). The results are consistent with what has been reported previously, *i.e.* inflammatory cell accumulation observed on day 3 and collagen deposition from day 7. A fibrous capsule can be seen from day 14 onwards.

As shown in Figure 3.5, silicon chips coated with dexamethasone-releasing composites negated the FBR for the 30-day implantation period. No accumulation of inflammatory cells or fibrous encapsulation was visible in any of the tissue samples.

The same observation has been made when the composites without silicon chips in their inner core were tested, as shown in Figure 3.6.

3.4. Discussion

Similarities between human and swine skin make the Gottingen minipig a good large animal model to investigate the prevention of FBR to subcutaneous implants[26]. In the previous chapter, it has been determined that minipigs require higher levels of dexamethasone released in the local microenvironment to prevent FBR compared to rats. In addition, the existence of a release lag phase between days 1 and 10 was detrimental to the anti-FBR effect of the composites in the minipig model but not in the rat models. In this work, we utilized the knowledge gained from our previous studies to develop a one-month dexamethasone-releasing composite coating that was capable of preventing FBR in minipigs.

Previously, dexamethasone has been encapsulated in PLGA microspheres by suspending micronized dexamethasone crystals in a PLGA solution and further emulsifying the suspension in an aqueous phase followed by organic solvent extraction and microsphere formation[23, 27, 28]. This formulation showed a lag phase in the one-month release profile[21, 29, 30]. It was hypothesized that the lag phase was due to poor drug distribution in the microsphere matrix and that improving the drug distribution would minimize the lag phase.

Instead of suspending dexamethasone crystals in the PLGA solution, a co-solvent system (DCM/DMSO) to dissolve both dexamethasone and PLGA in the oil phase was used. Further, the process parameters were adjusted to ensure that dexamethasone precipitates immediately before PLGA. This facilitated the encapsulation of dexamethasone as small crystals throughout the polymer matrix. The inclusion of DMSO in the outer water phase (30% v/v) was crucial in achieving this, as it slowed down the diffusion of DMSO from the oil to the water phase and thus the precipitation of dexamethasone. Moreover, the ratio of the co-solvents in the inner oil phase was crucial to achieving timely dexamethasone precipitation and was optimized at 4:1

DCM:DMSO by volume. Lastly, dilution of the emulsion in a large volume of water ensured that PLGA precipitated immediately after dexamethasone precipitation. These parameters were optimized by utilizing PLM to monitor drug precipitation during processing, as shown in Figure 3.1 and Figure 3.2.

The optimized microsphere formulation was incorporated into the PVA hydrogel and was tested for *in vitro* release. The composites were spiked with crystalline dexamethasone to accommodate the lack of dexamethasone release during the first 24 hours. This additional dexamethasone accounted for 40% of the total drug content of the composites. As expected, the free dexamethasone was released rapidly from the composites, with 40% release during the first 24 hours. This release is crucial to negating the acute inflammatory phase. A further 15% of dexamethasone was released during days 2 and 3, which is likely due to release of dexamethasone encapsulated near the surface of the microspheres or inside smaller microspheres. From day 4 until day 45, dexamethasone was constantly released at an approximately zero order rate (more than 90% cumulative drug release). The slight deviation from linearity ($R^2 = 0.9931$) during this release period may be due to the wide size distribution of the microspheres, with the smaller microspheres contributing more near the beginning of the release and the larger microspheres contributing more towards the end of the release profile. Another possible reason for this deviation from linearity is the degradation pattern of PLGA, which undergoes auto-catalyzed degradation through the generation of hydrogen ions that facilitate hydrolysis.

Composites made with the optimized PLGA formulation were tested in Goettingen minipigs for their efficacy in preventing the FBR for one month. It was determined that the FBR can be completely negated by the constant release of dexamethasone throughout the implantation period. In addition, implants made of composites with no silicon chips in their core (to allow for higher

dexamethasone loading) were investigated and it was shown that these also prevented FBR. The need for higher dexamethasone doses in minipigs compared to rats (which were the focus of previous research) is likely due to the highly collagenous nature of the swine subcutaneous tissue. This results in more severe and earlier appearance of fibrosis. While the *in vivo* studies were conducted for a period of 30 days, the *in vitro* release studies revealed dexamethasone release for 45 days. Accordingly, these composites may be useful to prevent FBR for more than 30 days, however, this has not yet been tested *in vivo* and will be part of future investigations.

3.5. Conclusions

A novel method for the preparation of microspheres containing insoluble drugs was developed to achieve homogeneous drug distribution, high loading and low burst release. Dexamethasone microspheres prepared by this method, together with crystalline dexamethasone, were utilized in microsphere/hydrogel composite coatings to achieve an approximately 40% burst release followed by a constant drug release pattern with no lag phase. This microsphere/hydrogel composite coating formulation successfully prevented FBR in a large animal model for a period of one month via localized release of low doses of dexamethasone (approximately 10 μg per day, which is close to 1000 times below the level that which would result in any systemic effects (0.75 to 9 mg per day). To the best of the authors' knowledge, this is the first time that such low doses of dexamethasone, suitable for miniaturized medical devices such as biosensors, have been used to prevent FBR in a large animal model.

3.6. References

1. Leppert, P.S. and J.A. Fix, *Subcutaneous tissue cages for examination of slow release of materials from long-term implants.* Biomaterials, 1990. **11**(1): p. 46-9.
2. Aebischer, P., et al., *Tissue reaction to fabrics coated with turbostratic carbon: subcutaneous versus vascular implants.* Biomaterials, 1988. **9**(1): p. 80-5.

3. Semmelink, J.M., et al., *Granuloma and plasma cell formation induced by the subcutaneous implantation of beta-whitlockite particles.* Biomaterials, 1986. **7**(2): p. 152-4.
4. Granstrom, L., L. Backman, and S.E. Dahlgren, *Tissue reaction to polypropylene and polyester in obese patients.* Biomaterials, 1986. **7**(6): p. 455-8.
5. Sugar, O. and O.T. Bailey, *Subcutaneous reaction to silicone in ventriculoperitoneal shunts. Long-term results.* J Neurosurg, 1974. **41**(3): p. 367-71.
6. Rigdon, R.H., *Inflammation associated with dacron and teflon: an experimental study in mice, rats and rabbits.* Tex Rep Biol Med, 1974. **32**(2): p. 535-51.
7. Rigdon, R.H., *Plastics and inflammation: an in vivo experimental study.* J Biomed Mater Res, 1974. **8**(2): p. 97-117.
8. Smahel, J., J. Moserova, and E. Behounkova, *Tissue reactions after subcutaneous implantation of Hydron Sponge.* Acta Chir Plast, 1971. **13**(4): p. 193-202.
9. Tsai, Y.T., et al., *Optical imaging of fibrin deposition to elucidate participation of mast cells in foreign body responses.* Biomaterials, 2014. **35**(7): p. 2089-96.
10. Butler, K., et al., *A comparison of fibrous tissue formation surrounding intraperitoneal and subcutaneous implantation of ALCAP, HA, and TCP ceramic devices.* Biomed Sci Instrum, 1997. **34**: p. 18-23.
11. Imber, G., et al., *Fibrous capsule formation after subcutaneous implanation of synthetic materials in experimental animals.* Plast Reconstr Surg, 1974. **54**(2): p. 183-6.
12. Bolgen, N., et al., *Tissue responses to novel tissue engineering biodegradable cryogel scaffolds: an animal model.* J Biomed Mater Res A, 2009. **91**(1): p. 60-8.
13. Kamelger, F.S., et al., *A comparative study of three different biomaterials in the engineering of skeletal muscle using a rat animal model.* Biomaterials, 2004. **25**(9): p. 1649-55.
14. Kirschbaum, M., H. Amon, and G. Jennemann, *[Histologic reactions following implantation of a "lyodura-soft" band--animal experiment studies of an abdomino-vaginal sling operation].* Zentralbl Gynakol, 1989. **111**(15): p. 1049-54.
15. Wang, Y., F. Papadimitrakopoulos, and D.J. Burgess, *Polymeric "smart" coatings to prevent foreign body response to implantable biosensors.* J Control Release, 2013. **169**(3): p. 341-7.
16. Nichols, S.P., et al., *The effect of nitric oxide surface flux on the foreign body response to subcutaneous implants.* Biomaterials, 2012. **33**(27): p. 6305-12.
17. Kolb, C.M., L.M. Pierce, and S.B. Roofe, *Biocompatibility comparison of novel soft tissue implants vs commonly used biomaterials in a pig model.* Otolaryngol Head Neck Surg, 2012. **147**(3): p. 456-61.
18. Radin, S., et al., *In vivo tissue response to resorbable silica xerogels as controlled-release materials.* Biomaterials, 2005. **26**(9): p. 1043-52.
19. Bhardwaj, U., et al., *PLGA/PVA hydrogel composites for long-term inflammation control following s.c. implantation.* Int J Pharm, 2010. **384**(1-2): p. 78-86.
20. Bhardwaj, U., et al., *Controlling acute inflammation with fast releasing dexamethasone-PLGA microsphere/pva hydrogel composites for implantable devices.* J Diabetes Sci Technol, 2007. **1**(1): p. 8-17.
21. Zolnik, B.S. and D.J. Burgess, *Evaluation of in vivo-in vitro release of dexamethasone from PLGA microspheres.* J Control Release, 2008. **127**(2): p. 137-45.
22. Patil, S.D., F. Papadmitrakopoulos, and D.J. Burgess, *Concurrent delivery of dexamethasone and VEGF for localized inflammation control and angiogenesis.* J Control Release, 2007. **117**(1): p. 68-79.
23. Patil, S.D., F. Papadimitrakopoulos, and D.J. Burgess, *Dexamethasone-loaded poly(lactic-co-glycolic) acid microspheres/poly(vinyl alcohol) hydrogel composite coatings for inflammation control.* Diabetes Technol Ther, 2004. **6**(6): p. 887-97.

24. Hickey, T., et al., *In vivo evaluation of a dexamethasone/PLGA microsphere system designed to suppress the inflammatory tissue response to implantable medical devices.* J Biomed Mater Res, 2002. **61**(2): p. 180-7.
25. Ward, W.K., et al., *Controlled release of dexamethasone from subcutaneously-implanted biosensors in pigs: localized anti-inflammatory benefit without systemic effects.* J Biomed Mater Res A, 2010. **94**(1): p. 280-7.
26. Rausch, L., et al., *Use of the domestic Swine as an alternative animal model for conducting dermal irritation/corrosion studies on fatty amine ethoxylates.* Int J Toxicol, 2003. **22**(4): p. 317-23.
27. Galeska, I., et al., *Controlled release of dexamethasone from PLGA microspheres embedded within polyacid-containing PVA hydrogels.* AAPS J, 2005. **7**(1): p. E231-40.
28. Hickey, T., et al., *Dexamethasone/PLGA microspheres for continuous delivery of an anti-inflammatory drug for implantable medical devices.* Biomaterials, 2002. **23**(7): p. 1649-56.
29. Zolnik, B.S., P.E. Leary, and D.J. Burgess, *Elevated temperature accelerated release testing of PLGA microspheres.* J Control Release, 2006. **112**(3): p. 293-300.
30. Shen, J. and D. J. Burgess (2012). "Accelerated in vitro release testing of implantable PLGA microsphere/PVA hydrogel composite coatings." Int J Pharm 422(1-2): 341-348.

Chapter 4

Prevention of the Foreign Body Reaction and Promotion of Angiogenesis around Subcutaneous Implants

Abstract

Dexamethasone-releasing PLGA poly(lactic-co-glycolic acid) microsphere/PVA (polyvinyl alcohol) hydrogel composite coatings have been shown to prevent the foreign body reaction (FBR) to subcutaneous implants in small and large animal models. Such coatings were developed to extend the lifetime of implantable biosensors. However, long-term exposure of tissue to low levels of dexamethasone results in a reduction in blood vessel density due to the anti-angiogenic effect of dexamethasone. This mild effect, while not threatening to the subject's health, may interfere with analyte detection and sensor response time over the long-term. VEGF has been previously incorporated into these coatings and the anti-angiogenic effect of dexamethasone was reduced. The present work focused on administration of combinations of three tissue response modifiers (TRMs), dexamethasone, VEGF and PDGF (platelet derived growth factor) which prevent the FBR, increase angiogenesis and promote blood vessel maturation (which increases blood flow), respectively. To minimize any potential interference among the three TRMs (for example, PDGF increases fibrosis), the relative doses of dexamethasone, VEGF and PDGF were adjusted. It was determined that: *a)* all three TRMs are required for maximum promotion of angiogenesis, blood vessel maturation and prevention of the FBR; *b)* VEGF has to be administered at higher doses than PDGF; *c)* an increase in dexamethasone dosing must be accompanied by a proportional increase in growth factor dosing; and *d)* modification of the TRM ratio can achieve a constant capillary density throughout the implantation period which is important for applications such as biosensors to maintain sensitivity and a stable sensor baseline.

4.1. Introduction

Biosensors, defined as analytical devices that detect biological analytes, have progressed in their development and miniaturization such that fully-implantable sensors (usually in the subcutaneous tissue) will become a reality in the near future[1-12]. These sensors will provide real-time, continuous monitoring of analytes, such as glucose, which are currently being monitored intermittently. Diabetic patients are a major group that will benefit from the realization of implantable biosensors, since tight blood glucose control is paramount to diabetic health.

Once implanted, biosensors are attacked by the body's defense mechanism, a cascade of events collectively known as the foreign body reaction (FBR) which results in the encapsulation of biosensors in a fibrous membrane that isolates them from the surrounding tissue and thus renders them ineffective[13, 14]. The FBR and its prevention have been a research focus during the past decades; the most common method to prevent the FBR is by the continuous administration of an anti-inflammatory agent, most commonly dexamethasone[6, 13-16]. Dexamethasone is popular due to its high efficacy and potency which result in only small amounts of the drug being required for long-term action. However, long-term exposure of a tissue to low levels of dexamethasone results in reduction in blood vessel density in the local area due to dexamethasone's anti-angiogenic effect[17-19]. This mild effect, while not detrimental to the subject's health, may interfere with analyte detection and sensor the response time.

Glucose diffuses passively from the blood to the subcutaneous tissue where it can be detected by an implanted biosensor. The time it takes for glucose to travel from the capillary wall to the sensor surface is dependent on the distance it has to cover, and typically ranges from 6 to 15 minutes[20]. Long-term exposure of dexamethasone decreases the number of capillaries available for glucose diffusion to the sensor, as well as increases the average distance between the capillaries

and the sensor surface. Both effects may significantly increase sensor response lag time as well as sensitivity. Accordingly, growth factors that promote angiogenesis can be administered alongside dexamethasone in order to prevent dexamethasone-induced ischemia and reduce glucose sensor lag times. VEGF (vascular endothelial growth factor) has successfully been administered with dexamethasone through poly(lactic-co-glycolic acid) (PLGA) microspheres embedded in a polyvinyl alcohol (PVA) hydrogel over a one-month period and an increase in capillary density was observed[21]. To further increase the capillary density around the implants, the current work focuses on administration of dexamethasone, VEGF and PDGF (platelet derived growth factor). VEGF promotes the migration of endothelial cells to the site, which form new branches on existing blood vessels[22-25]. PDGF promotes the maturation of the new branches by attracting pericytes that form an outer cellular layer on the new branches and connect venous and arterial blood flow[26-29].

It is known that angiogenesis and the FBR have some mechanistic overlap; cytokines that promote branching of existing blood vessels and recruitment of endothelial cells (primarily VEGF) exacerbate acute inflammation and inhibit chronic inflammation (which starts with the activation of fibroblasts)[30-32]. On the other hand, cytokines that promote the maturation of new blood vessel branches (primarily PDGF), *via* the recruitment of pericytes, promote chronic inflammation[33-36]. In addition, dexamethasone is well known to inhibit angiogenesis. It is therefore evident that the simultaneous release of these three molecules in a tissue will result in significant interference in their respective roles. In the current work, composite implants containing combinations of dexamethasone, VEGF and PDGF were investigated in the subcutaneous tissue using a rat model. The tissue surrounding the implants was examined *via* histological evaluation for prevention of the FBR and concurrent promotion of angiogenesis. Adjustment of the relative ratios of the three

TRMs eliminated interference among the TRMs that was observed for some of the composite combinations.

4.2. Materials and Methods

4.2.1. Materials

Dexamethasone was purchased from Cayman Chemical Company (Ann Arbor, MI). VEGF, PDGF and their respective ELISA quantification kits were purchased from Peprotech (Rocky Hill, NJ). High-molecular weight polyvinyl alcohol (HMW-PVA, MW 133 kDa), was purchased from Polysciences, Inc. (Warrington, PA). Low-molecular weight PVA (LMW-PVA, 99% hydrolyzed, MW 30-700 kDa), bovine serum albumin (BSA), and BSA-FITC were purchased from Sigma-Aldrich (St. Louis, MO). PLGA Resomer® RG503H (inherent viscosity 0.32–0.44 dl/g) was a gift from Boehringer-Ingelheim. Methylene chloride was purchased from Fisher Scientific (Pittsburghm, PA). Sprague Dawley rats were purchased from Charles River Laboratories (Willimantic, CT).

4.2.2. Formulation of protein microspheres

In a 50-ml Teflon vial, 500 mg of PLGA were added with 2 ml methylene chloride (DCM). After the polymer was dissolved, 200 μl of the protein phase (100 mg/ml BSA with either 5 μg VEGF (V_MS), 5 μg PDGF (P_MS) or 5 μg VEGF and 2.5 μg PDGF (VP_MS)) were added to the polymer solution. The vial was vortexed at 3,000 rpm for 10 seconds and homogenized at 10,000 rpm for 30 seconds to achieve a water-in-oil primary emulsion. A secondary water-in-oil-in-water emulsion was made by adding 10 ml water phase (1% w/v of LMW-PVA, with or without 2% w/v NaCl) and vortexing at 3,000 rpm for 10 seconds. The secondary emulsion was diluted with 10 ml of Milli-Q water to speed up polymer precipitation and microsphere formation. The

diluted emulsion was kept under vacuum on a horizontal shaker at 300 rpm for 3 hours. The hardened microspheres were purified to remove LMW-PVA and non-encapsulated drug *via* three centrifugation cycles (2 min, 3,500 rpm), freeze dried overnight and stored at -20°C until further use. Formulations containing 2% w/w FITC-BSA (of the total BSA amount) were prepared to visualize the protein distribution inside the microspheres. All microsphere preparation steps took place in a single vial (from polymer dissolution in the organic solvent to microsphere storage), as demonstrated in Figure 4.1.

4.2.3. Formulation of dexamethasone microspheres

Dexamethasone-containing microspheres were prepared as above with the 200 μl protein solution replaced by 100 mg of crystalline dexamethasone. A homogenous drug suspension in the polymer solution was achieved following 2.5 min of homogenization at 10,000 rpm.

4.2.4. Microsphere characterization

Drug loading (dexamethasone): 5 mg of dried microspheres were dissolved in 1 ml DMSO and then diluted 10 times in phosphate buffered saline (PBS) pH 7.4. Dexamethasone concentration was determined *via* RP-HPLC (PerkinElmer, Inc.). Mobile phase 35% acetonitrile in water, 0.1% phosphoric acid; column C18 500x03 mm; and detection wavelength 240 nm.

Drug loading (growth factors): 2 mg of dried microspheres were dissolved in 1 ml acetone, and the undissolved pellets were washed and collected *via* three centrifugation cycles (12,000 rpm, 5 min) and dried under vacuum for 30 min to remove acetone. The pellets, which contained the proteins, were reconstituted in 1 ml of PBS containing 0.1% Tween 20. VEGF and PDGF ELISA kits were used to quantify the growth factor concentration in the reconstituted solutions, as per the manufacturer's instructions.

Particle size: An Accusizer 780 (Particle Sizing Systems) was used to measure the particle size of the PLGA microspheres. 3-5 mg of dried microspheres were suspended in 1 ml of 0.1% w/v LMW PVA solution, bath-sonicated for 10 seconds to break any aggregates and analyzed for volume-based average size.

Confocal microscopy: A Nikon A1R Spectral confocal microscope was used to visualize protein distribution inside the microspheres. Microspheres were suspended in distilled water prior to imaging, and FITC-BSA was detected at excitation and emission wavelengths of 494 and 518 nm, respectively.

4.2.5. Fabrication of composites

A predetermined amount of PLGA microspheres were added to 1 ml of HMW-PVA solution in water (5% w/v) and the mixture was bath-sonicated for 10 seconds to achieve a homogenous suspension. The suspension was fed into stainless steel tubes with inner diameter 1.5 mm and subjected to three freeze-thaw cycles (2 h at -20°C, 1 h at ambient temperature) to physically cross-link the HMW-PVA solution to form a hydrogel. The gels were removed from the tubes and cut at 5 mm length pieces, air-dried for 3 hours and stored at -20°C until further use. The different groups of composites prepared and their compositions are shown in Table 4.1.

4.2.6. Investigation of VEGF-to-PDGF ratio

Spraque Dawley rats (male, 150-200 g) were used as a small animal model (6 per group). Each rat was implanted with composites C, D, DV, DVP, and D2VPa (as defined in Table 4.1 above) on the dorsal area. Each member of a group of rats was implanted with four composites of the same type. Implants were spaced at least 2 cm apart to ensure no interference. Rats were euthanized 30 days after implantation. After euthanasia, the composites with surrounding subcutaneous tissue

and skin were removed and fixed in 10% buffered formalin solution for 24 hours. They were then processed at UConn's pathobiology services, embedded in paraffin blocks and cut into 20 μm-thick sections. The samples were immune-stained against smooth muscle actin (sma), which stains mature blood vessels.

4.2.7. Investigation of dexamethasone-to-growth factor ratio

Based on the outcome of the growth factor ratio study, this investigation included composites D, DV, D2VPb as well as one with a higher dexamethasone dose (2D2VP). The study design was as described above with the following differences: Rats were euthanized on different days in groups of 6 (day 3, 7, 14, 21, and 30 following implantation). In addition to immune-staining against sma, the samples from the final study were also stained using a standard H&E protocol to monitor the anti-FBR effect of the composites. Anti-sma-stained tissue slides were examined *via* light microscopy, and the total number of capillaries within a distance of 200 μm around the implants were blind-counted, and the average values and standard deviations were calculated from three samples.

All animal studies were reviewed and approved by the University of Connecticut's Institutional Animal Care and Use Committee.

4.3. Results

4.3.1. Microsphere preparation and characterization

Protein distribution inside the PLGA microspheres was optimized in a pilot study (using only BSA as model protein). 2% w/v of NaCl was added to the outer water phase to induce removal of the inner water phase through osmosis while leaving the protein molecules inside the polymer matrix. The microspheres were characterized for protein distribution, drug loading and burst

release. It was determined that by incorporation of NaCl in the outer water phase, protein distribution in the microsphere matrix improved significantly and the burst release was reduced, as shown in Figure 4.2.

Dexamethasone- and growth factor-loaded PLGA microspheres were prepared with the optimized method described above, and were characterized for drug loading and particle size as shown in Table 4.2.

4.3.2. VEGF-to-PDGF ratio

The relative amounts of VEGF and PDGF were changed while dexamethasone dosing was kept constant. Figure 4.3 shows tissue samples around composites C, D, DV, DVP, D2VPa, as well as normal tissue (N) away from implantation sites at 30 days following implantation. Mature blood vessel walls stained red. As expected, control implants (C) with no dexamethasone, VEGF or PDGF, showed fibrosis (blue band around the implant). Implants D, which were loaded with dexamethasone but no growth factors, showed no fibrosis, and the blood vessel density around these implants was significantly lower than that of normal tissue. Implants DVP, which were loaded with equal amounts of VEGF and PDGF showed fibrosis and low blood vessel density near the surface of the implants. Implants D2VPa with a VEGF and PDGF ratio of 2:1 showed angiogenesis, with capillaries oriented around the implant.

4.3.3. Adjustment of dexamethasone dose

Based on the results of the previous study, implants D, DV, D2VPb and 2D2VP were used to investigate their anti-FBR effect throughout a one-month period. Figure 4.4 shows representative tissue sections from day 3 to day 30 following implantation for the different composites. No inflammation (infiltration of inflammatory cells present on day 3 and fibrotic band present from

day 14 onwards) was observed in any of the composites. This was expected for composites D which have previously been studied for their anti-FBR effect and were used as a control here. Composites that contained VEGF or combinations of VEGF and PDGF in addition to dexamethasone also showed no inflammation. In the combination composites (D2VPb and 2D2VP), dexamethasone was loaded at two doses to confirm that the minimum effective dose previously determined for composites with only dexamethasone and VEGF is effective in the combination coatings.

Figure 4.5 shows the angiogenic effect of the composites 7, 14, 21 and 30 days following implantation at a low magnification (10x). Higher-magnification (40x) images are shown in Figure 4.6 and the capillary density around the implants was quantified as reported in Figure 4.7. The highest angiogenesis throughout the implantation period was achieved with composites D2VPb ($P<0.001$ compared to the control group), and the capillaries were oriented around the implant. Composites D2VPb were the only composites with capillaries around their entire perimeter, as shown in Figure 4.5.

4.4. Discussion

Accurate quantification of angiogenesis in the subcutaneous tissue is challenging, and different approaches have been applied by research groups depending on each application[37-41]. For example, in studies where ischemia was investigated in large parts of a tissue, the perfusion of the tissue (blood volume reaching a specific area) was measured *via* imaging techniques such as ultra-sound[42, 43]. For applications that investigated small tissue areas, such as in the studies reported here, histological evaluation is the most common method of assessment of angiogenesis. In the current studies, angiogenesis was monitored *via* immune-staining against sma, which is present on the surface of mature blood vessels (vessels with connected venous and arterial branches)[44-46].

Since the delivery system presented here was developed for implantable biosensors, the area nearest to the implant (200 μm from the implant surface) was utilized in counting blood capillaries. This quantification approach revealed significant increase in capillary density in the immediate vicinity of the implant for composites with the three-TRM combinations. In addition, it is important to consider the capillary size and distribution around the implants since these factors will affect the total amount of glucose reaching the implant surface and the spatial distribution of glucose in the tissue, respectively. Accordingly, low- and high-magnification images of the tissue surrounding the implant were analyzed.

Biosensors rely on analytes (*e.g.* glucose) to diffuse from the blood to the subcutaneous tissue and reach the sensor surface for their functionality. It has been reported previously that concurrent release of dexamethasone and VEGF can prevent the FBR and promote angiogenesis over the long-term in rats[21]. In this work, dexamethasone, VEGF and PDGF were delivered simultaneously and their relative doses were adjusted to achieve the highest capillary density at minimal distance from the implant surface while eliminating interference between the angiogenic and anti-inflammatory effects of these three TRMs.

Initially, the dexamethasone dose was kept constant (at the dose previously optimized to prevent FBR for implants coated with composites containing only dexamethasone) and the relative VEGF and PDGF amounts were varied. It was determined that delivering equal amounts of VEGF and PDGF alongside dexamethasone interfered with the anti-FBR effect of the latter, and a fibrotic band was observed around the implant (DVP). In addition, no new capillaries developed close to the implant; this is probably due to the presence of the fibrotic band obstructing subsequent VEGF and PDGF release to the local tissue. It was determined that reducing the amount of PDGF loaded in the implants by half (D2VPa) eliminated interference with the anti-FBR effect of

dexamethasone, and significant increase in blood vessel density was observed compared to the control group (D).

Based on these results, the VEGF-to-PDGF ratio was kept constant at 2:1, and both growth factors were loaded in a single population of microspheres in this ratio (VP_MS). To study the extent of the interference between the three TRMs, a higher dexamethasone dose was investigated. It was determined that the anti-FBR effect of the implants remained intact, while the capillary density was reduced and the average capillary-to-implant distance was increased. This indicates that in order to preserve the angiogenic effect of such composites at higher dexamethasone doses, the growth factor dose needs to be increased proportionally.

In the interest of improving biosensor functionality (lag time and sensitivity), it is important to note that the formulation that showed maximum angiogenic effect (D2VPb) also had a higher capillary density at day 30 compared to the other time points. This variation may potentially affect biosensor functionality in terms of stable baseline readings. However, this variation in capillary density with time did not occur in formulation 2D2VP (which had a higher dexamethasone dose).

4.5. Conclusions

In this work, combinations of dexamethasone, VEGF and PDGF were delivered for the first time to prevent FBR and promote angiogenesis. Visual examination of histological images at low and high magnifications combined with capillary density measurements around the implants was necessary for data interpretation. It was determined that: *i)* prevention of FBR along with maximum angiogenesis around the implants requires all three TRMs in specific relative amounts; *ii)* VEGF has to be administered at higher doses than PDGF; *iii)* an increase in dexamethasone dosing reduces the angiogenic effect of the composites and must be accompanied by a proportional

increase in growth factor dosing; and *iv)* capillary density throughout the implantation period is a potential factor that may affect biosensor lag time and sensitivity.

4.6. References

1. Chiu, N.F., et al., *An implantable multifunctional needle type biosensor with integrated RF capability.* Conf Proc IEEE Eng Med Biol Soc, 2005. **2**: p. 1933-6.
2. Valdes, T.I. and F. Moussy, *In vitro and in vivo degradation of glucose oxidase enzyme used for an implantable glucose biosensor.* Diabetes Technol Ther, 2000. **2**(3): p. 367-76.
3. Vaddiraju, S., et al., *Microsphere erosion in outer hydrogel membranes creating macroscopic porosity to counter biofouling-induced sensor degradation.* Anal Chem, 2012. **84**(20): p. 8837-45.
4. Vaddiraju, S., et al., *Design and fabrication of a high-performance electrochemical glucose sensor.* J Diabetes Sci Technol, 2011. **5**(5): p. 1044-51.
5. Vaddiraju, S., et al., *Enhanced glucose sensor linearity using poly(vinyl alcohol) hydrogels.* J Diabetes Sci Technol, 2009. **3**(4): p. 863-74.
6. Wang, Y., et al., *Effect of dexamethasone-loaded poly(lactic-co-glycolic acid) microsphere/poly(vinyl alcohol) hydrogel composite coatings on the basic characteristics of implantable glucose sensors.* J Diabetes Sci Technol, 2012. **6**(6): p. 1445-53.
7. Croce, R.A., Jr., et al., *Theoretical analysis of the performance of glucose sensors with layer-by-layer assembled outer membranes.* Sensors (Basel), 2012. **12**(10): p. 13402-16.
8. Vaddiraju, S., et al., *The role of H2O2 outer diffusion on the performance of implantable glucose sensors.* Biosens Bioelectron, 2009. **24**(6): p. 1557-62.
9. Vaddiraju, S., et al., *Technologies for continuous glucose monitoring: current problems and future promises.* J Diabetes Sci Technol, 2010. **4**(6): p. 1540-62.
10. Vaddiraju, S., et al., *Hierarchical multifunctional composites by conformally coating aligned carbon nanotube arrays with conducting polymer.* ACS Appl Mater Interfaces, 2009. **1**(11): p. 2565-72.
11. Vaddiraju, S. and K.K. Gleason, *Selective sensing of volatile organic compounds using novel conducting polymer-metal nanoparticle hybrids.* Nanotechnology, 2010. **21**(12): p. 125503.
12. Vaddiraju, S., et al., *Emerging synergy between nanotechnology and implantable biosensors: a review.* Biosens Bioelectron, 2010. **25**(7): p. 1553-65.
13. Wang, Y., F. Papadimitrakopoulos, and D.J. Burgess, *Polymeric "smart" coatings to prevent foreign body response to implantable biosensors.* J Control Release, 2013. **169**(3): p. 341-7.
14. Morais, J.M., F. Papadimitrakopoulos, and D.J. Burgess, *Biomaterials/tissue interactions: possible solutions to overcome foreign body response.* AAPS J, 2010. **12**(2): p. 188-96.
15. Bhardwaj, U., et al., *Controlling acute inflammation with fast releasing dexamethasone-PLGA microsphere/pva hydrogel composites for implantable devices.* J Diabetes Sci Technol, 2007. **1**(1): p. 8-17.
16. Hickey, T., et al., *In vivo evaluation of a dexamethasone/PLGA microsphere system designed to suppress the inflammatory tissue response to implantable medical devices.* J Biomed Mater Res, 2002. **61**(2): p. 180-7.
17. Moura, S.A., et al., *Local drug delivery system: inhibition of inflammatory angiogenesis in a murine sponge model by dexamethasone-loaded polyurethane implants.* J Pharm Sci, 2011. **100**(7): p. 2886-95.
18. Nakao, S., et al., *Dexamethasone inhibits interleukin-1beta-induced corneal neovascularization: role of nuclear factor-kappaB-activated stromal cells in inflammatory angiogenesis.* Am J Pathol, 2007. **171**(3): p. 1058-65.

19. Luo, J.C., et al., *Dexamethasone delays ulcer healing by inhibition of angiogenesis in rat stomachs.* Eur J Pharmacol, 2004. **485**(1-3): p. 275-81.
20. Novak, M.T., F. Yuan, and W.M. Reichert, *Modeling the relative impact of capsular tissue effects on implanted glucose sensor time lag and signal attenuation.* Anal Bioanal Chem, 2010. **398**(4): p. 1695-705.
21. Patil, S.D., F. Papadmitrakopoulos, and D.J. Burgess, *Concurrent delivery of dexamethasone and VEGF for localized inflammation control and angiogenesis.* J Control Release, 2007. **117**(1): p. 68-79.
22. Ward, W.K., et al., *Vascularizing the tissue surrounding a model biosensor: how localized is the effect of a subcutaneous infusion of vascular endothelial growth factor (VEGF)?* Biosens Bioelectron, 2003. **19**(3): p. 155-63.
23. Poldervaart, M.T., et al., *Prolonged presence of VEGF promotes vascularization in 3D bioprinted scaffolds with defined architecture.* J Control Release, 2014. **184**: p. 58-66.
24. Celik-Ozenci, C., et al., *Expressions of VEGF and its receptors in rat corpus luteum during interferon alpha administration in early and pseudopregnancy.* Mol Reprod Dev, 2004. **67**(4): p. 414-23.
25. Flamme, I., G. Breier, and W. Risau, *Vascular endothelial growth factor (VEGF) and VEGF receptor 2 (flk-1) are expressed during vasculogenesis and vascular differentiation in the quail embryo.* Dev Biol, 1995. **169**(2): p. 699-712.
26. Caplan, A.I. and D. Correa, *PDGF in bone formation and regeneration: new insights into a novel mechanism involving MSCs.* J Orthop Res, 2011. **29**(12): p. 1795-803.
27. Stratman, A.N., et al., *Endothelial-derived PDGF-BB and HB-EGF coordinately regulate pericyte recruitment during vasculogenic tube assembly and stabilization.* Blood, 2010. **116**(22): p. 4720-30.
28. Hellberg, C., A. Ostman, and C.H. Heldin, *PDGF and vessel maturation.* Recent Results Cancer Res, 2010. **180**: p. 103-14.
29. Abramsson, A., P. Lindblom, and C. Betsholtz, *Endothelial and nonendothelial sources of PDGF-B regulate pericyte recruitment and influence vascular pattern formation in tumors.* J Clin Invest, 2003. **112**(8): p. 1142-51.
30. Kajdaniuk, D., et al., *Vascular endothelial growth factor (VEGF) - part 1: in physiology and pathophysiology.* Endokrynol Pol, 2011. **62**(5): p. 444-55.
31. Zittermann, S.I. and A.C. Issekutz, *Endothelial growth factors VEGF and bFGF differentially enhance monocyte and neutrophil recruitment to inflammation.* J Leukoc Biol, 2006. **80**(2): p. 247-57.
32. Kirk, S.L. and S.J. Karlik, *VEGF and vascular changes in chronic neuroinflammation.* J Autoimmun, 2003. **21**(4): p. 353-63.
33. Bonner, J.C., *Regulation of PDGF and its receptors in fibrotic diseases.* Cytokine Growth Factor Rev, 2004. **15**(4): p. 255-73.
34. Cao, B., et al., *The potential role of PDGF, IGF-1, TGF-beta expression in idiopathic pulmonary fibrosis.* Chin Med J (Engl), 2000. **113**(9): p. 776-82.
35. Bonner, J.C., et al., *Induction of PDGF receptor-alpha in rat myofibroblasts during pulmonary fibrogenesis in vivo.* Am J Physiol, 1998. **274**(1 Pt 1): p. L72-80.
36. Wangoo, A., et al., *Up-regulation of alveolar macrophage platelet-derived growth factor-B (PDGF-B) mRNA by interferon-gamma from Mycobacterium tuberculosis antigen (PPD)-stimulated lymphocytes.* Clin Exp Immunol, 1993. **94**(1): p. 43-50.
37. Shi, P., et al., *Automated computational framework of blood vessel quantification in chick chorioallantoic membrane angiogenesis.* J Biomed Opt, 2014. **19**(10): p. 106005.
38. AlMalki, W.H., et al., *Assessment methods for angiogenesis and current approaches for its quantification.* Indian J Pharmacol, 2014. **46**(3): p. 251-6.

39. Ungersma, S.E., et al., *Vessel imaging with viable tumor analysis for quantification of tumor angiogenesis.* Magn Reson Med, 2010. **63**(6): p. 1637-47.
40. Boettcher, M., T. Gloe, and C. de Wit, *Semiautomatic quantification of angiogenesis.* J Surg Res, 2010. **162**(1): p. 132-9.
41. Low, Q.E. and L.A. DiPietro, *Quantification of wound angiogenesis.* Methods Mol Med, 2003. **78**: p. 319-27.
42. Ge, W., Y. Zheng, and Z. Tao, *Contrast-enhanced ultrasound analysis of tissue perfusion in tumor-bearing mice following treatment with endostatin combined with radiotherapy.* Exp Ther Med, 2014. **7**(5): p. 1359-1363.
43. Rissanen, T.T., et al., *High-resolution ultrasound perfusion imaging of therapeutic angiogenesis.* JACC Cardiovasc Imaging, 2008. **1**(1): p. 83-91.
44. Kurz, H., et al., *Pericytes in the mature chorioallantoic membrane capillary plexus contain desmin and alpha-smooth muscle actin: relevance for non-sprouting angiogenesis.* Histochem Cell Biol, 2008. **130**(5): p. 1027-40.
45. Brey, E.M., et al., *Three-dimensional, quantitative analysis of desmin and smooth muscle alpha actin expression during angiogenesis.* Ann Biomed Eng, 2004. **32**(8): p. 1100-7.
46. Rogers, P.A., D. Plunkett, and B. Affandi, *Perivascular smooth muscle alpha-actin is reduced in the endometrium of women with progestin-only contraceptive breakthrough bleeding.* Hum Reprod, 2000. **15 Suppl 3**: p. 78-84.

Chapter 5

Continuous Metabolic Monitoring Based on Multi-Analyte Biomarkers to Predict Exhaustion

Abstract

This work introduces the concept of multi-analyte biomarkers for continuous metabolic monitoring. The importance of using more than one marker lies in the ability to obtain a holistic understanding of the metabolism. This is showcased for the detection and prediction of exhaustion during intense physical exercise. The findings presented here indicate that when *glucose* and *lactate* changes over time are combined into multi-analyte biomarkers, their monitoring trends are more sensitive in the subcutaneous tissue, an implantation-friendly peripheral tissue, compared to the blood. This unexpected observation was confirmed in normal as well as type 1 diabetic rats. This study was designed to be of direct value to continuous monitoring biosensor research, where single analytes are typically monitored. These findings can be implemented in new multi-analyte continuous monitoring technologies for more accurate insulin dosing, as well as for exhaustion prediction studies based on objective data rather than the subject's perception.

5.1. Introduction

Metabolic monitoring is the periodic recording of metabolic markers that give information on specific metabolic pathways. Diabetes mellitus, obesity and intense physical activity are a few examples where close metabolic monitoring is necessary[1-3]. This is routinely done in a non-continuous manner, where the individual records their blood glucose, body weight, blood pressure, *etc.* over various periods of time. Technological advances on wearable and/or implantable devices have initiated the transition to real-time, continuous monitoring[4-8]. However, monitoring devices have several shortcomings: they trigger the foreign body reaction which results in loss of functionality within a few days, they cannot be implanted directly in the bloodstream, and they typically record only single analytes. The foreign body reaction to implantable medical devices has been shown to be prevented by incorporating drug-eluting biocompatible coatings[8-10]. When a device that is implanted in a peripheral tissue such as subcutaneous tissue is used to monitor analyte changes in the blood, loss of sensitivity and lag times are observed[11]. This is due to the fact that analytes have to diffuse from the bloodstream to the interstitial fluid before being detected.

Exhaustion, also known as fatigue, is the inability of muscle to continue an ongoing physical activity[12]. The perception of exhaustion is highly subjective, and consequently the assessment of a subject's endurance is currently based on semi-empirical observations that link the fitness and current state (*e.g.* heart rate) of each subject with pre-recorded performance levels[13,14]. However, exhaustion has been linked to several metabolic pathways and therefore a close examination of the metabolic processes involved in physical activity could facilitate a more accurate prediction of exhaustion. Depletion of fuel stored in the muscle (*i.e.* creatine and glycogen, that are readily accessible as an energy source), as well as accumulation of metabolic byproducts (*e.g.* chloride and potassium ions and lactic acid) are considered the causes of exhaustion[15,16]. These metabolic

events take place in the exercising muscle, a body compartment that is not available for real-time, continuous monitoring *via* implantable devices mainly due to the trauma associated with intramuscular implantations.

In this work, exhaustion detection in the subcutaneous tissue using multiple analytes combined into multi-analyte biomarkers was investigated. Single-analyte monitoring, such as glucose monitoring, creates blind spots in the recorded metabolic state since a single analyte cannot account for all pathways involved in a given metabolic event. It is hypothesized that monitoring of two analytes (glucose and lactate) will offer a more complete view into metabolic changes during exercise that lead up to exhaustion. In the context of exhaustion prediction, glucose and lactate are suitable candidates for multi-analyte monitoring: glucose is the primary energy source of muscle cells, and lactate is the main by-product of anaerobic metabolism during intense activity.

To test the above hypothesis, exercise experiments were conducted in normal as well as type 1 diabetic rats. Diabetic rats were included in the study design since one application of this work will be to improve the health of diabetic athletes. External observations (commencement of exercise, running speed, and onset of exhaustion) were correlated with internal shifts in metabolism (glucose and lactate as single readings or combined into multi-analyte biomarkers) recorded in the subcutaneous tissue and the blood. Microdialysis was used to monitor glucose and lactate in the subcutaneous tissue and the blood. Microdialysis is a reliable technique that has been used extensively in laboratory settings to monitor analyte changes in various tissues.

5.2. Materials and Methods

5.2.1. Animal models

Male Sprague Dawley rats (6 weeks old, 150-170 g) were used as the normal animal model (n=6). One group of rats was injected with streptozotocin (60 mg/kg body weight, IP) to induce

type 1 diabetes (n=3). Additionally, Zucker Diabetic Fatty (ZDF) rats, an obesity animal model, were used in the preliminary studies (n=3). However, data from ZDF rats were not included in this manuscript since these animals could not perform intense exercise due to their physical condition. All animal studies were done in accordance with the approved guidelines. All studies were reviewed and approved by the University of Connecticut's Institutional Animal Care and Use Committee (IACUC) prior to the beginning of the experiments.

5.2.2. Microdialysis

Microdialysis was used to monitor analytes in the blood and subcutaneous tissue. Each rat was implanted with one microdialysis catheter (20 kDa molecular weight cut-off, CMA Microdialysis AB) in the subcutaneous tissue and one in the jugular vein. Catheterization took place with the aid of a guiding needle as per the manufacturer's instructions.

5.2.3. Exercise experiments

Rats implanted with two microdialysis catheters were placed in a forced exercise treadmill (IITC, Inc.). An isotonic liquid (Ringer's solution) was pumped through the microdialysis catheters at 5 μl/min speed rate (syringe pump, Harvard Apparatus) and samples were collected every 10 minutes (preliminary studies) and every 6 minutes for the all other studies. After an initial resting period to collect baseline data, exercise commenced at maximum running speed. The maximum speed varied with each rat and was in the range of 15-17 meters per minute. The onset of exhaustion was noted when the rats could not keep up at the maximum pace, and the exercise ended when the rats failed to run at all. A recovery period was allowed after the exercise.

5.2.4. Analyte quantification

YSI 2300 STAT Plus™ (YSI Life Sciences, Inc.) was used to quantify glucose and lactate molar concentrations in the microdialysis samples. Oxygen and carbon dioxide microelectrodes

(Microelectrodes, Inc.) were used to determine analyte trends in the microdialysis samples. Since oxygen and carbon dioxide monitoring was found unsuitable for this application, only the electrode output is reported to obtain the analyte trend.

5.2.5. Data analysis

Analyte concentrations were plotted against time as shown in the main text of the manuscript. With the exception of the exhaustion prediction times (which are reported as average values ± standard deviation), animal data could not be aggregated for statistical analysis due to variability on the fitness and endurance level of each rat. Representative plots of analyte trends are shown to showcase the feasibility of multi-analyte biomarkers for exhaustion prediction.

5.3. Results

5.3.1. Choice of analytes to be monitored

Glucose and lactate were chosen as markers based on preliminary studies where blood and subcutaneous glucose, lactate, oxygen and carbon dioxide were monitored in healthy and obese animals during light exercise. The results indicated that oxygen and carbon dioxide are not suitable analytes for predicting exhaustion. As shown in Figure 5.1, oxygen trends did not respond to light exercise while carbon dioxide values were highly unstable.

5.3.2. Glucose and lactate changes during intense exercise

Figure 5.2a depicts a representative metabolic profile for a healthy rat. Glucose and lactate changes in the blood and subcutaneous tissue are shown in four zones. *A:* prior to exercise (baseline measurements); *B:* during intense exercise; *C:* during light exercise (post-exhaustion); and *D:* recovery. Since glucose and lactate have to diffuse from the blood to the subcutaneous tissue to be taken up by the microdialysis catheter, the small differences in blood and subcutaneous values were expected. A spike in both glucose and lactate levels in the blood as well as the subcutaneous

tissue are observed upon commencement of exercise, a typical observation when transitioning from rest to activity. Exhaustion was first observed 57 minutes into the exercise, when the animal could not keep up and the treadmill speed had to be adjusted. Full exhaustion was observed 30 minutes later, when the animal was unable to continue the exercise. Interestingly, glucose and lactate showed a trend change around 45 minutes into the exercise, 12 minutes before the first physical evidence of exhaustion and 42 minutes before full exhaustion (indicated by red ovals). The exhaustion-prediction window varied from 12 to 20 minutes among the rats, due to varied endurance levels. The average exhaustion prediction time was 16.17 ± 4.16 min.

Similar observations of exhaustion prediction were made in untreated, type 1 diabetic rats (Figure 5.2b) with an average exhaustion prediction time of 8.60 ± 3.08 min. However, diabetic rats did not show a gradual manifestation of exhaustion, but reached full exhaustion immediately. As shown in Figure 5.2b, glucose as well as lactate build-up was observed. The type 1 diabetic rats were untreated (they did not receive insulin injections). As a result, glucose released from the liver as an energy source could not be internalized by muscle cells which failed to perform the exercise shortly after glucose and lactate build-up stopped. It should be noted that the data from diabetic rats exhibited one anomaly: the glucose values obtained from the microdialysis samples were consistently lower than the values obtained from normal rats. This conflicted with glucose values obtained *via* tail vein pricking to confirm the diabetic state (>350 mg/dL). However, the interpretation of the data shown here relies on the trend rather than the absolute values of glucose and lactate, and this anomaly did not interfere with data interpretation.

The findings described above confirmed our hypothesis that detectable metabolic changes precede physical manifestations of exhaustion. Accordingly, these changes may be used as a predictive tool for exercise endurance and exhaustion.

5.3.3. Multi-analyte biomarker identification

The observations described above are based on blood levels of glucose and lactate (monitored independently) as these changes were not as evident in the subcutaneous tissue. This poses a potential problem in translating these findings into subcutaneously-implantable monitoring platforms. It was hypothesized that by combining glucose and lactate readings into multi-analyte biomarkers it may be possible to increase the monitoring resolution in the subcutaneous tissue since glucose and lactate account for aerobic and anaerobic metabolism, respectively. Glucose (GLU) and lactate (LAC) combinations were investigated. Since one glucose molecule yields two lactate molecules, the lactate concentration was used directly or multiplied by two to account for this. The efficacy of the biomarkers to increase the monitoring resolution in the subcutaneous tissue was tested by measuring the absolute slope changes during two metabolic events: rest-to-activity transition (first peak in Figures 5.2a and 5.2b) and pre-exhaustion trend changes (second peak in Figures 5.2a and 5.2b). It was determined that combinations of biomarkers were several times more sensitive to metabolic changes in the subcutaneous tissue compared to the blood as shown in Figure 3a for normal rats and Figure 3b for diabetic rats. Single analyte changes relative to the baseline measurements (%CLU and %LAC) also showed higher sensitivity in the subcutaneous tissue than the blood. The utilization of percent changes of single analytes is not feasible for continuous monitoring systems as stable baseline measurements are not usually available outside controlled laboratory environments. This is especially relevant for individuals undergoing fitness level changes (due to training or disease management) whose metabolic baseline is continuously shifting, as well as subjects with no control over their activity levels such as deployed military personnel.

5.3.4. Multi-analyte biomarkers for prediction of exhaustion

Based on the results shown in Figures 5.3a and 5.3b, *2LAC/GLU* was plotted *vs.* time for normal and diabetic rats (Figure 5.4a). As shown in this figure, *2LAC/GLU* can be used to predict exhaustion with more accuracy in the subcutaneous tissue than the blood. 3D surface plots of glucose, lactate, and time were constructed (Figure 5.4b). These plots incorporate all possible combinations of glucose and lactate and when implemented into standardized exercise routines[17-27] can provide feedback on the fitness and endurance of the subject. As shown in Figure 5.4b, the exhaustion-predictive metabolic changes described above in response to exercise are more profound in areas where glucose and lactate are combined compared to the peripheral regions of the graph where glucose and lactate are plotted separately.

Discussion

This work explored the potential of the subcutaneous tissue, a device implantation-friendly space, to be used in continuous metabolic monitoring for exhaustion prediction. The ultimate goal is to utilize the proof-of-concept presented here to develop exhaustion-predicting algorithms that rely on holistic metabolic shifts instead of single markers such as heart rate or lactate. An array of biomarkers that can be used in such algorithms was successfully identified, and furthermore the concept of constructing 3D biomarker plots was presented.

Continuous monitoring of more than one analyte can reveal the interdependence of different metabolic pathways and the metabolic flexibility of the individual (the ability to switch from aerobic to anaerobic utilization of energy and vice versa). Our findings revealed that multi-analyte biomarkers based on glucose and lactate are far more responsive in the subcutaneous tissue (an implantation-friendly compartment) than in the blood. This is a significant breakthrough for subcutaneously-implanted monitoring devices since until now their inability to detect analytes directly in the blood was considered a handicap.

The size and shape of the semi-implantable microdialysis probe makes it a good model for implantable biosensors. In the future, when implantable multi-sensors become available, the concept of continuous multi-analyte monitoring for exhaustion prediction presented here will be applied to individualized algorithms paired with such devices. The applications of this concept are many. Long-term changes in multi-analyte biomarker interdependence are expected to reveal progress in the training of athletes, management of diabetic patients, development of pre-diabetes in obese subjects, *etc*. Here it was shown that multi-analyte biomarkers can be used to predict exhaustion, which is crucial for diabetic athletes, deployed military personnel, and other high-risk individuals involved in intense physical activity.

5.5. References

1 Greenhill, C. Diabetes: Regular self-monitoring of blood glucose needed for metabolic control. *Nature reviews. Endocrinology* **6**, 417, doi:10.1038/nrendo.2010.98 (2010).

2 Mader, J. K. *et al.* Microdialysis--a versatile technology to perform metabolic monitoring in diabetes and critically ill patients. *Diabetes research and clinical practice* **97**, 112-118, doi:10.1016/j.diabres.2012.02.010 (2012).

3 Stuckey, M. *et al.* Remote monitoring technologies for the prevention of metabolic syndrome: the Diabetes and Technology for Increased Activity (DaTA) study. *Journal of diabetes science and technology* **5**, 936-944 (2011).

4 Croce, R. A., Jr. *et al.* A miniaturized transcutaneous system for continuous glucose monitoring. *Biomedical microdevices* **15**, 151-160, doi:10.1007/s10544-012-9708-x (2013).

5 Turner, A. P. & Pickup, J. C. Diabetes mellitus: biosensors for research and management. *Biosensors* **1**, 85-115 (1985).

6 Vaddiraju, S., Burgess, D. J., Jain, F. C. & Papadimitrakopoulos, F. The role of H2O2 outer diffusion on the performance of implantable glucose sensors. *Biosensors & bioelectronics* **24**, 1557-1562, doi:10.1016/j.bios.2008.08.015 (2009).

7 Vaddiraju, S., Burgess, D. J., Tomazos, I., Jain, F. C. & Papadimitrakopoulos, F. Technologies for continuous glucose monitoring: current problems and future promises. *Journal of diabetes science and technology* **4**, 1540-1562 (2010).

8 Wang, Y., Papadimitrakopoulos, F. & Burgess, D. J. Polymeric "smart" coatings to prevent foreign body response to implantable biosensors. *Journal of controlled release : official journal of the Controlled Release Society* **169**, 341-347, doi:10.1016/j.jconrel.2012.12.028 (2013).

9 Bhardwaj, U., Sura, R., Papadimitrakopoulos, F. & Burgess, D. J. Controlling acute inflammation with fast releasing dexamethasone-PLGA microsphere/pva hydrogel composites for implantable devices. *Journal of diabetes science and technology* **1**, 8-17 (2007).

10 Hickey, T., Kreutzer, D., Burgess, D. J. & Moussy, F. In vivo evaluation of a dexamethasone/PLGA microsphere system designed to suppress the inflammatory tissue response to implantable

medical devices. *Journal of biomedical materials research* **61**, 180-187, doi:10.1002/jbm.10016 (2002).

11 Vaddiraju, S., Singh, H., Burgess, D. J., Jain, F. C. & Papadimitrakopoulos, F. Enhanced glucose sensor linearity using poly(vinyl alcohol) hydrogels. *Journal of diabetes science and technology* **3**, 863-874 (2009).

12 Hawley, J. A. & Reilly, T. Exhaustion revisited. *Journal of sports sciences* **15**, 245-246, doi:10.1080/026404197367245 (1997).

13 Calik-Kutukcu, E. *et al.* A comparison of muscle strength and endurance, exercise capacity, exhaustion perception and quality of life in patients with chronic obstructive pulmonary disease and healthy subjects: a cross-sectional study. *BMC pulmonary medicine* **14**, 6, doi:10.1186/1471-2466-14-6 (2014).

14 Myles, W. S. Sleep deprivation, physical exhaustion, and the perception of exercise intensity. *Medicine and science in sports and exercise* **17**, 580-584 (1985).

15 Ishii, H. & Nishida, Y. Effect of Lactate Accumulation during Exercise-induced Muscle Exhaustion on the Sensorimotor Cortex. *Journal of physical therapy science* **25**, 1637-1642, doi:10.1589/jpts.25.1637 (2013).

16 Roschel, H., Gualano, B., Marquezi, M., Costa, A. & Lancha, A. H., Jr. Creatine supplementation spares muscle glycogen during high intensity intermittent exercise in rats. *Journal of the International Society of Sports Nutrition* **7**, 6, doi:10.1186/1550-2783-7-6 (2010).

17 Burr, J. F. *et al.* Relationship of physical fitness test results and hockey playing potential in elite-level ice hockey players. *Journal of strength and conditioning research / National Strength & Conditioning Association* **22**, 1535-1543, doi:10.1519/JSC.0b013e318181ac20 (2008).

18 Jones, S. B., Knapik, J. J., Sharp, M. A., Darakjy, S. & Jones, B. H. The validity of self-reported physical fitness test scores. *Military medicine* **172**, 115-120 (2007).

19 Knapik, J. J., Hauret, K. G., Lange, J. L. & Jovag, B. Retention in service of recruits assigned to the army physical fitness test enhancement program in basic combat training. *Military medicine* **168**, 490-492 (2003).

20 Mitchell, T., White, E. D., 3rd & Ritschel, D. Investigating the correlation of the U.S. Air Force Physical Fitness Test to combat-based fitness: a women-only study. *Military medicine* **179**, 653-658, doi:10.7205/MILMED-D-13-00445 (2014).

21 Worden, T. & White, E. D., 3rd. Modifying the U.S. Air Force Fitness Test to reflect physical combat fitness: one study's perspective. *Military medicine* **177**, 1090-1094 (2012).

22 Calogiuri, G., Weydahl, A. & Sothern, R. B. Heart rate response to a standardized walking exercise in the Arctic circumpolar region in morning vs. evening during the polar night and midnight sun. *The Journal of sports medicine and physical fitness* **51**, 444-451 (2011).

23 Garrigue, S. *et al.* Performance of a rate responsive accelerometer-based pacemaker with autocalibration during standardized exercise and recovery. *Pacing and clinical electrophysiology : PACE* **25**, 883-887 (2002).

24 Hareendran, A. *et al.* Proposing a standardized method for evaluating patient report of the intensity of dyspnea during exercise testing in COPD. *International journal of chronic obstructive pulmonary disease* **7**, 345-355, doi:10.2147/COPD.S29571 (2012).

25 Hayes, D. L., Von Feldt, L. & Higano, S. T. Standardized informal exercise testing for programming rate adaptive pacemakers. *Pacing and clinical electrophysiology : PACE* **14**, 1772-1776 (1991).

26 Lindholm, E., Brevinge, H., Bergh, C. H., Korner, U. & Lundholm, K. Relationships between self-reported health related quality of life and measures of standardized exercise capacity and metabolic efficiency in a middle-aged and aged healthy population. *Quality of life research : an international journal of quality of life aspects of treatment, care and rehabilitation* **12**, 575-582 (2003).

27 Terziyski, K., Marinov, B., Hodgev, V., Tokmakova, M. & Kostianev, S. Standardized peak exercise perception score: validation of a new index of effort perception. *Journal of cardiopulmonary rehabilitation and prevention* **30**, 40-46, doi:10.1097/HCR.0b013e3181c85a26 (2010).

Chapter 6

Conclusions and Future Studies

6.1. Summary and conclusions

There are currently a number of semi-implantable biosensors on the market that monitor glucose continuously; these devices, however, lose functionality after 6-10 days due to the tissue reaction to the implanted (needle-like) portion of the device. As a result, to this day, continuous glucose monitoring has not been implemented into routine diabetes management. Consequently, there is a great need for a biosensor that *i)* functions for prolonged periods of time and *ii)* has minimal interference with the daily life of diabetic patients to enable patient compliance. Such a biosensor will revolutionize diabetes management with additional applicability in the fields of exercise metabolism as well as remote health monitoring in the military.

To achieve long-term sensor functionality *in vivo*, modification of the tissue reaction to implanted biosensors is necessary. A significant amount of research has led to the realization of biosensor coatings that prevent the FBR and prolong sensor lifetime *in vivo*. These coatings had previously been tested in small animal models (normal and diabetic rats). Accordingly, the main scope of this work was to transfer the technology from small to large animals, expand the coating functionality to promote angiogenesis alongside prevention of FBR, and explore applications of sensors in exercise physiology.

Key differences in the FBR to subcutaneous implants between a small (rat) and large (minipig) animal model were identified for the first time. The onset and severity of fibrosis was determined to be a significant difference, with minipigs demonstrating earlier onset and more severe chronic inflammation compared to rats. It was determined that dexamethasone release from the implant

coatings must be tailored to the species-specific stages of the FBR. In order to counter the more severe chronic inflammation observed in minipigs compared to rats, dexamethasone release must be continuous, with no lag phase. The effective dexamethasone dosing regime was 100 μg during the first day and 10 μg/day thereafter; this regime is applicable to implants of similar size (7 x 0.15 mm) and can be extrapolated to longer implantation periods in minipigs. These findings can facilitate the dose calculations in the first-in-human studies as porcine skin is the optimal animal model for dermal formulations.

The species differences that were identified in the first part of this work were utilized to develop a novel method for the preparation of microspheres containing insoluble drugs with homogeneous drug distribution, high loading and low burst release. Dexamethasone microspheres prepared by this method, together with crystalline dexamethasone, were incorporated in microsphere/hydrogel composite coatings to achieve an approximately 40% burst release followed by a constant drug release pattern with no lag phase. This microsphere/hydrogel composite coating formulation successfully prevented FBR in a large animal model for a period of one month *via* localized release of low doses of dexamethasone (approximately 10 μg per day, which is close to 1000 times below the level that would result in any systemic effects (0.75 to 9 mg per day). This is the first time that such low doses of dexamethasone, suitable for miniaturized medical devices such as biosensors, have been used to prevent FBR in a large animal model.

In order to expand the effects of the composite coatings, combinations of dexamethasone, VEGF and PDGF were delivered for the first time to prevent FBR and promote angiogenesis in a rat model. Visual examination of histological images at low and high magnifications combined with capillary density measurements around the implants was necessary for data interpretation. It was determined that: *i)* prevention of FBR along with maximum angiogenesis around the implants

requires all three TRMs in specific relative amounts; *ii)* VEGF has to be administered at higher doses than PDGF; *iii)* an increase in dexamethasone dosing reduces the angiogenic effect of the composites and must be accompanied by a proportional increase in growth factor dosing; and *iv)* capillary density throughout the implantation period is a potential factor that may affect biosensor lag time and sensitivity.

Lastly, this work explored the potential of the subcutaneous tissue, a device implantation-friendly space, to be used in continuous metabolic monitoring for exhaustion prediction. The ultimate goal is to utilize the proof-of-concept presented here to develop exhaustion-predicting algorithms that rely on holistic metabolic shifts instead of single markers such as heart rate or lactate. An array of biomarkers that will be used in such algorithms was successfully identified, and furthermore the concept of constructing 3D biomarker plots was presented. It was determined that physical exhaustion is preceded by metabolic changes that can be picked up *via* continuous monitoring of glucose and lactate in the subcutaneous tissue, indicating that prediction of exhaustion with an approximately 14-minute window is possible. This will be of paramount importance for deployed soldiers, diabetic athletes and other high-risk individuals involved in intense physical activity.

The significant and novel contributions resulting from this work include: *i)* identification of key species differences between the FBR in small and large animals; *ii)* development of a novel dexamethasone-loaded microsphere fabrication method to accommodate the identified species differences; *iii)* prevention of the FBR in a large animal model using small amounts of anti-inflammatory drug release; *iv)* development of a innovative, single-vessel protein microsphere preparation method with enhanced efficiency, product recovery, and sterility; *v)* application of osmosis to encapsulate proteins in polymer microspheres; *vi)* delivery of dexamethasone, VEGF,

and PDGF to prevent FBR while promoting angiogenesis in a rat model; *vii)* adjustment of the three TRM dose ratios to eliminate interference in their respective actions; *ix)* application of continuous, multi-analyte monitoring to predict exhaustion in normal and diabetic rats; and *x)* introduction of multi-analyte biomarkers for metabolic monitoring in the subcutaneous tissue with higher sensitivity than the blood.

The above contributions will advance the field of metabolic monitoring *via* implantable biosensors by transferring the technology in large animals for pre-clinical testing, expanding the sensor lifetime to three months with the use of angiogenic growth factors, and identifying important biomarkers that can be incorporated in metabolic monitoring algorithms.

6.2. Future studies

The novel microsphere fabrication methods developed here (dexamethasone-loaded and protein-loaded presented in Chapters 3 and 4, respectively) have been successfully tested *in vivo*. Different drugs (small and large molecules) can be encapsulated with these methods to expand the potential applications of these microspheres. For example, the osmosis-driven microsphere preparation method can be modified to include both small and large molecules, whereas the drug-polymer co-precipitation method can be further investigated for longer drug release periods.

So far, the electrochemical elements of the sensors were optimized based on testing in small animals. The biosensor coatings developed and used here to prevent FBR in large animals can be used in large animal sensor testing. Such testing is necessary in order to transition to the first-in-human studies of coated implantable biosensors.

It was demonstrated here that adjustment of dexamethasone, VEGF, and PDGF dose ratios eliminate their interference for one month implantation periods. This effect may be studied for

longer periods, such as three and six months. It is expected that the ratio that works for one month will be effective for longer periods as well, however, this needs to be confirmed *via* careful examination of longer-releasing formulations. In addition, composites that release dexamethasone, VEGF, and PDGF have not been used in sensor testing studies. The effect of the capillary density as well as the capillary distance from the sensor surface has to be studied against sensor functionality in the long-term.

The importance of multi-analyte monitoring for exhaustion prediction has been demonstrated here. The next step will translate the ability of such biomarkers to predict exhaustion into algorithms that can be incorporated in biosensors. Rigorous validation of such algorithms in normal as well as diabetic animals will pave the way for human studies. In addition, multi-analyte monitoring may be applied to study other metabolic diseases such as obesity.

Appendix I – Figures

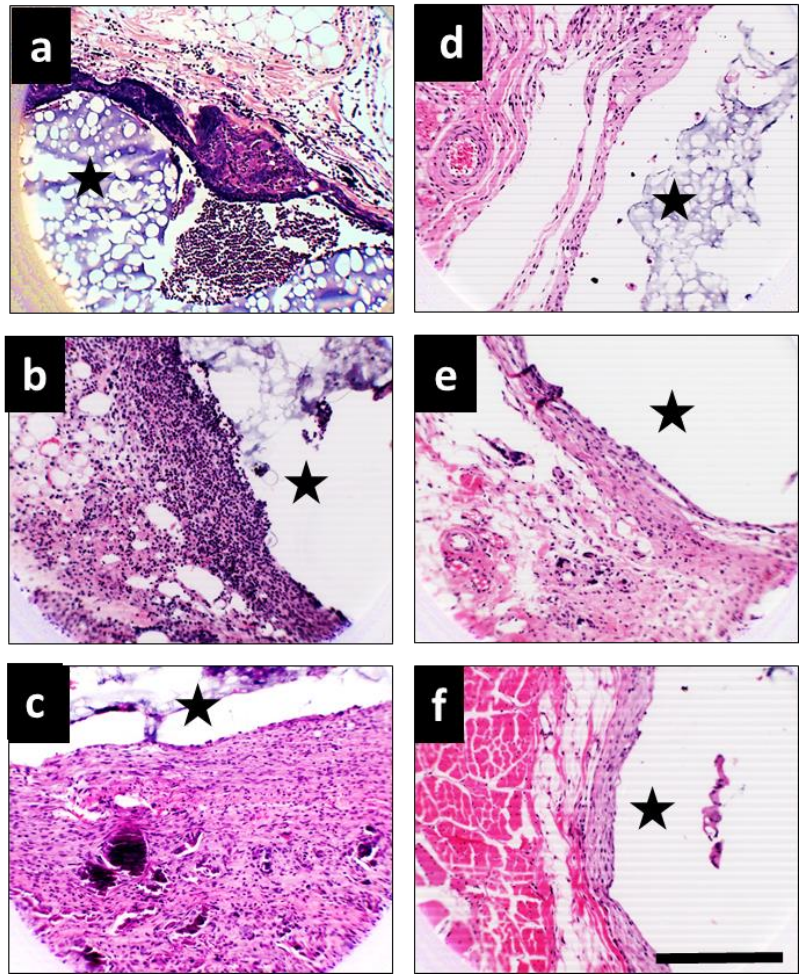

Figure 2.1. Histological evaluation of the foreign body reaction to control (no dexamethasone) implants. Star denotes implant location. Connective tissue is stained pink, collagen fibers light pink and inflammatory cells purple (H&E staining). *a*: day 1; *b*: day 3; *c*: day 7; *d*: day 14; *e*: day 21; *f*: day 30 post-implantation (n=3). Scale bar: 500 μm.

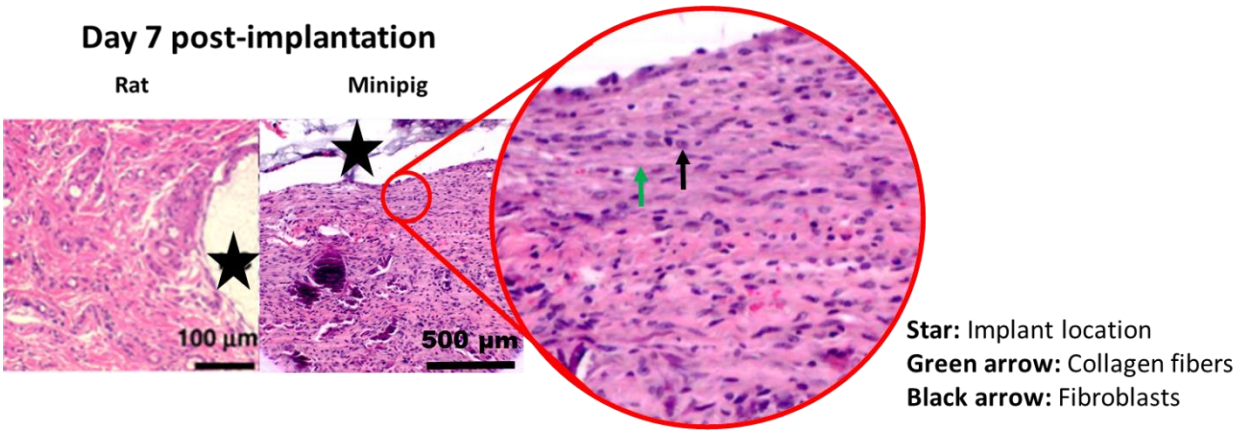

Figure 2.2. Comparison of FBR in rats and minipigs 7 days post-implantation. Star denotes implant location. Connective tissue is stained pink, collagen fibers light pink and inflammatory cells purple (H&E staining). Green arrow: collagen fibers; black arrow: fibroblasts. Rat image taken from Patil *et. al.*43 Fibroblasts were identified based on the cell morphology. Active fibroblasts have oval shape with spherical nucleus and are characteristically positioned in-between collagen fibers which they produce.

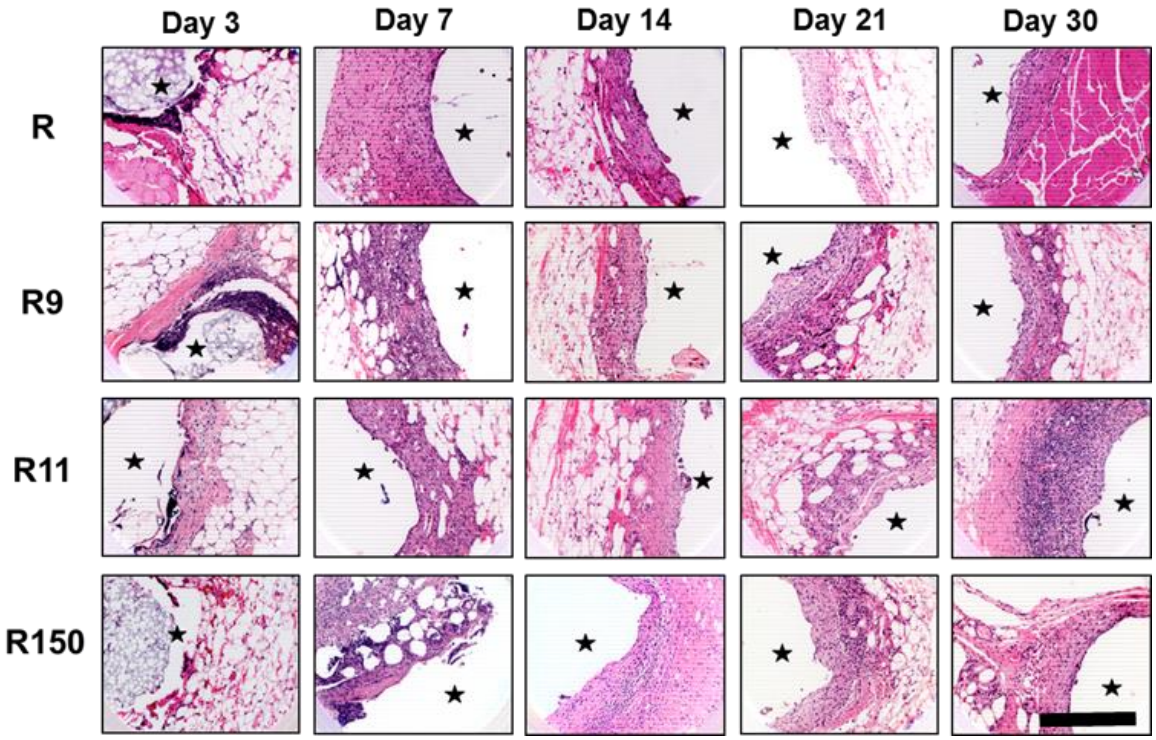

Figure 2.3. Histological evaluation of the foreign body reaction to dexamethasone-releasing implants R, R9, R11 and R150 on days 3, 7, 14, 21, and 30 post-implantation. Star denotes implant location. Connective tissue is stained pink, collagen fibers light pink and inflammatory cells purple (H&E staining) (n=3). Scale bar: 500 μm.

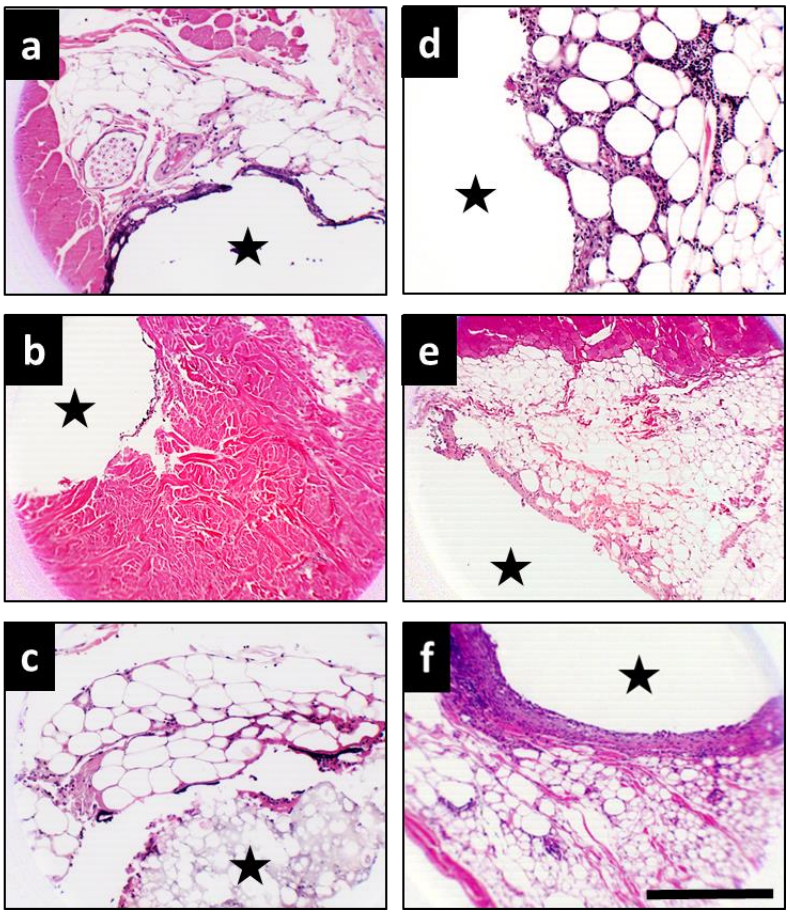

Figure 2.4. Histological evaluation of the foreign body reaction to dexamethasone-releasing implants R2W. Star denotes implant location. Connective tissue is stained pink, collagen fibers light pink and inflammatory cells purple (H&E staining). *a*: day 1; *b*: day 3; *c*: day 7; *d*: day 11; *e*: day 14; *f*: day 21 post-implantation (n=4). Scale bar: 500 µm.

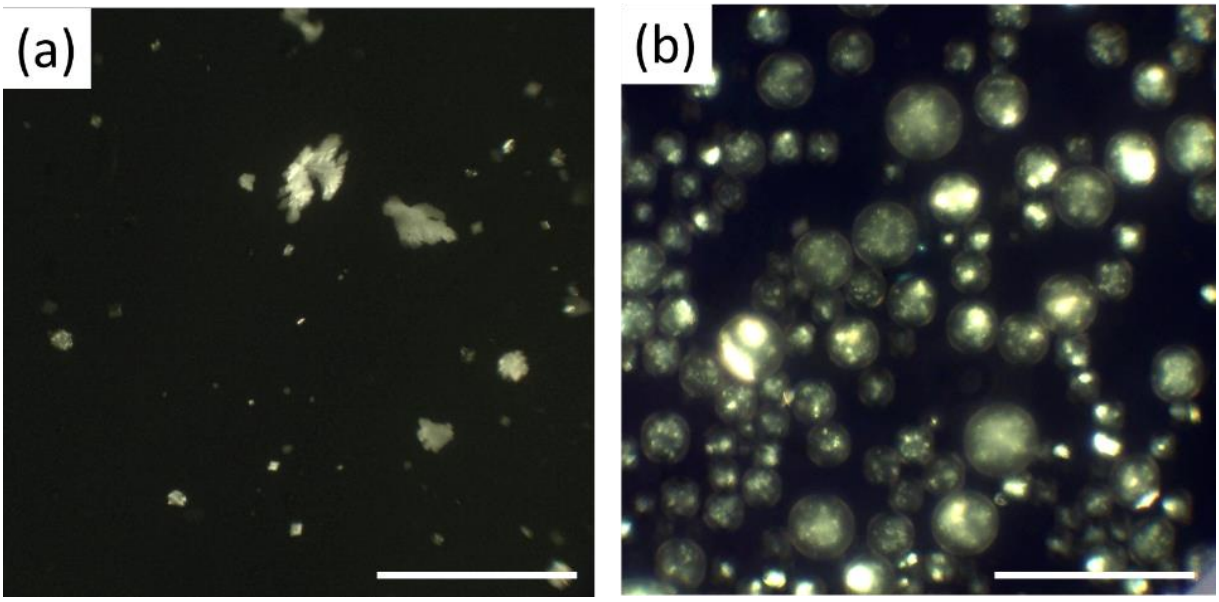

Figure 3.1. Polarized light microscopy (PLM) images of two emulsions during PLGA microsphere preparation. Drug crystals appear as bright spots in the PLM images. *(a)* Example of non-optimized process, with dexamethasone crystals formed outside the polymer phase (polymer droplets not visible due to their inability to polarize light). *(b)* Optimized formulation with dexamethasone precipitated inside the polymer phase. Magnification: 10X, scale bar: 500 μm.

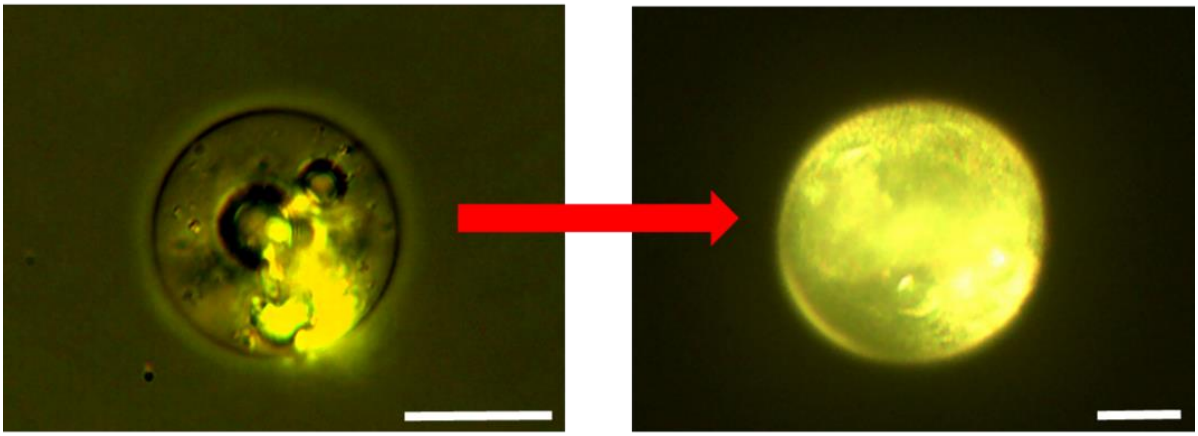

Figure 3.2. PLM images of negative control formulation (left) with poor drug distribution in the polymer matrix and optimized formulation (right). Dexamethasone crystals appear bright under PLM while the polymer is transparent. Magnification: 40X, scale bars: 10 μm.

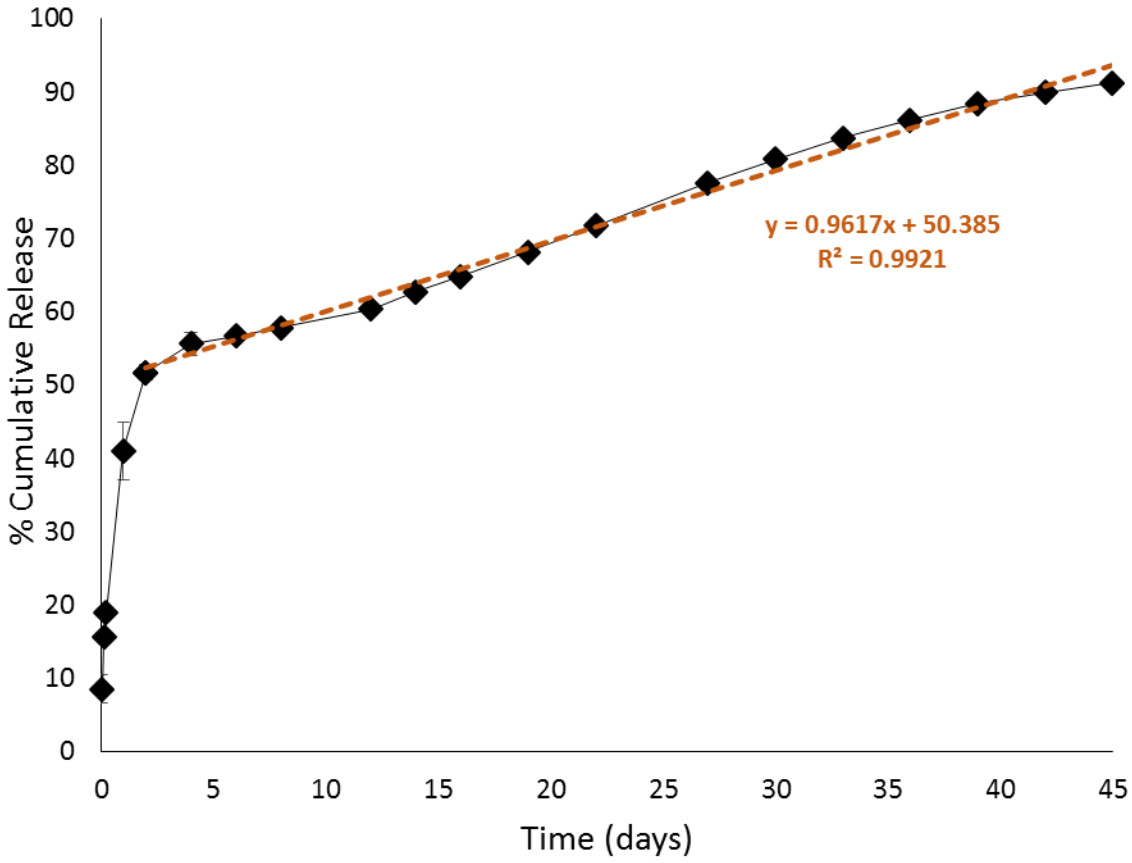

Figure 3.3. Cumulative *in vitro* release of dexamethasone from optimized PLGA microspheres embedded in a PVA hydrogels. All values are average ± SD (n = 3). Linear regression was applied from day 4 to day 45.

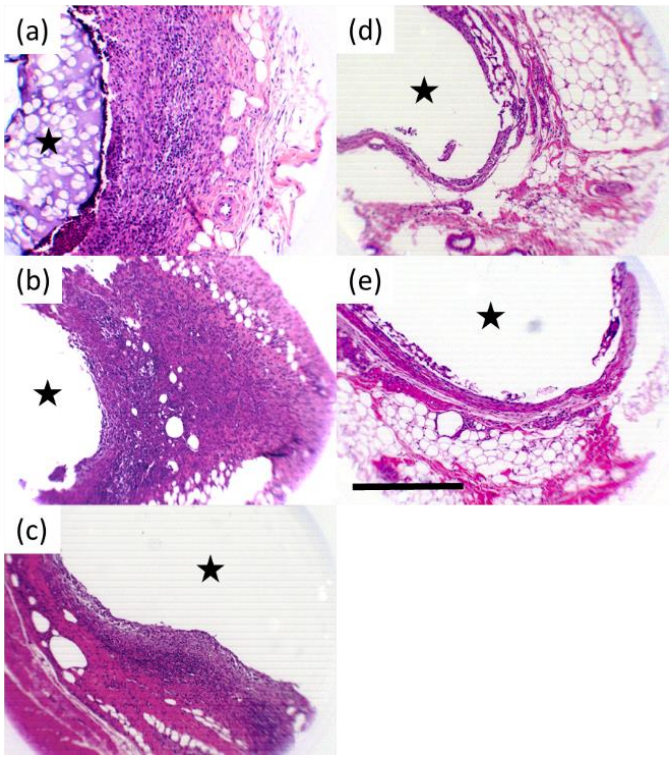

Figure 3.4. Histological evaluation of the foreign body reaction to control (no dexamethasone) implants. Star denotes implant location. Connective tissue is stained pink, collagen fibers light pink and inflammatory cells purple (H&E staining). *(a)* day 3; *(b)* day 7; *(c)* day 14; *(d)* day 21; *(e)* day 30 post-implantation. Magnification: 10X, scale bar: 500 μm.

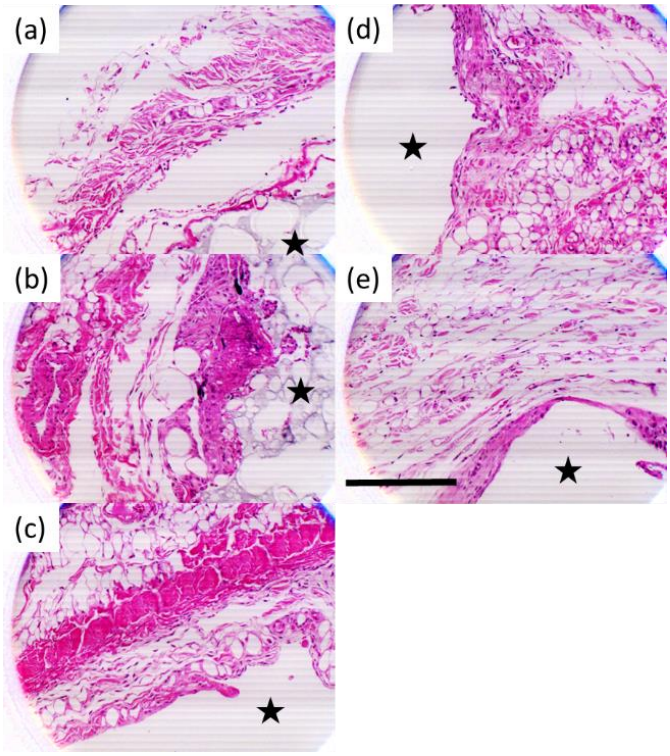

Figure 3.5. Histological evaluation of the foreign body reaction to coated silicon chips with the optimized PLGA microsphere formulation. Star denotes implant location. Connective tissue is stained pink, collagen fibers light pink and inflammatory cells purple (H&E staining). *(a)* day 3; *(b)* day 7; *(c)* day 14; *(d)* day 21; *(e)* day 30 post-implantation. Magnification: 10X, scale bar: 500 μm.

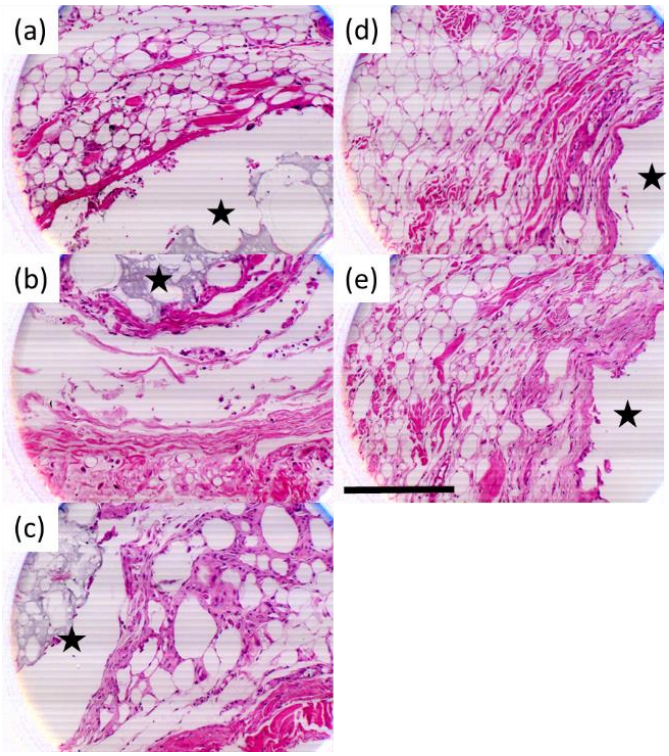

Figure 3.6. Histological evaluation of FBR to composites with the optimized PLGA microsphere formulation with no silicon chips at their core. Star denotes implant location. Connective tissue is stained pink, collagen fibers light pink and inflammatory cells purple (H&E staining). *(a)* day 3; *(b)* day 7; *(c)* day 14; *(d)* day 21; *(e)* day 30 post-implantation. Magnification: 10X, scale bar: 500 μm.

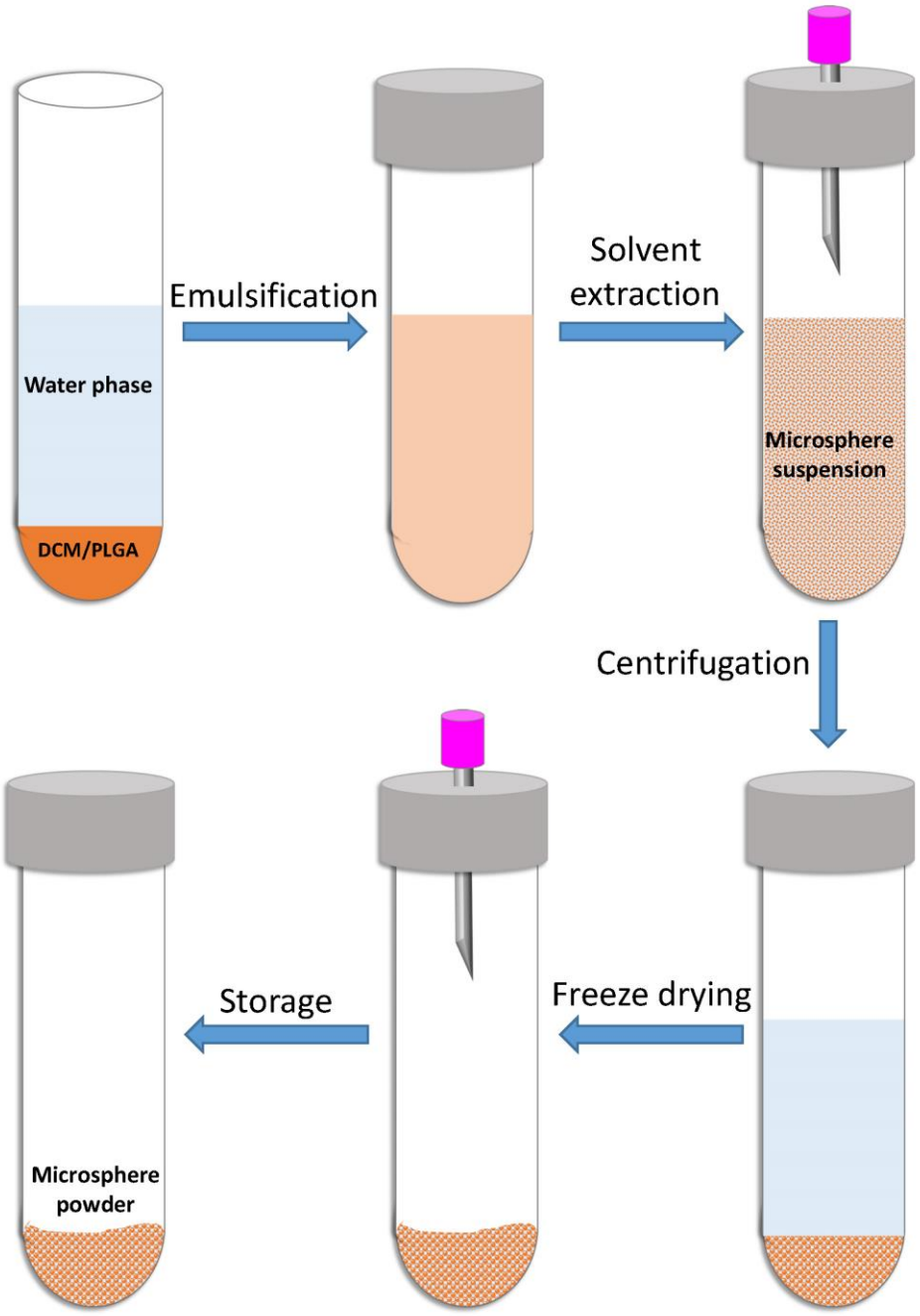

Figure 4.1. Schematic representation of the single-vessel microsphere preparation process.

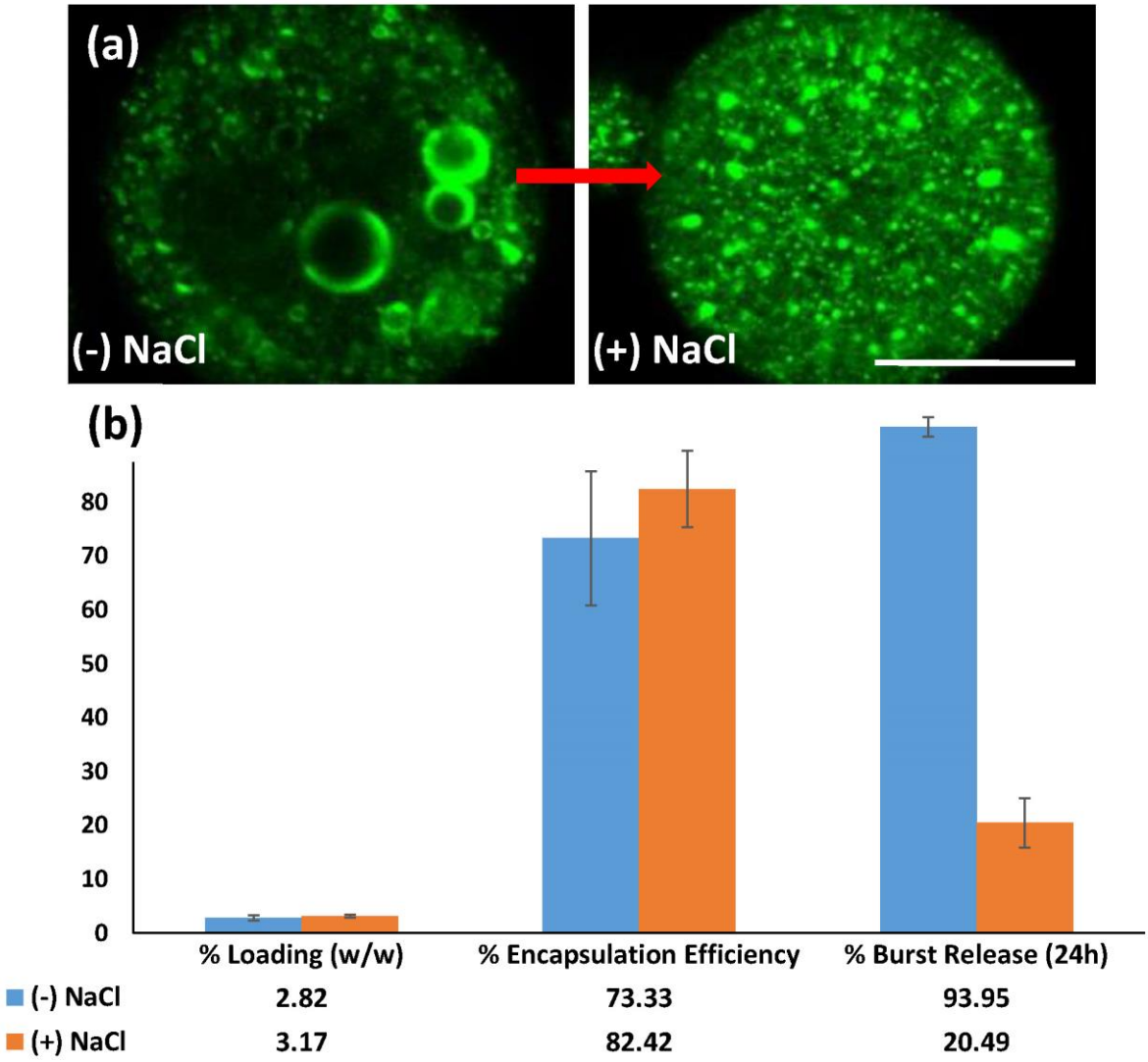

Figure 4.2. a) Confocal microscopy images of protein microsphere formulations with (right) and without (left) NaCl in the outer water phase; b) drug loading, encapsulation efficiency, and % burst release of the formulations with and without NaCl (mean ± SD, n=3).

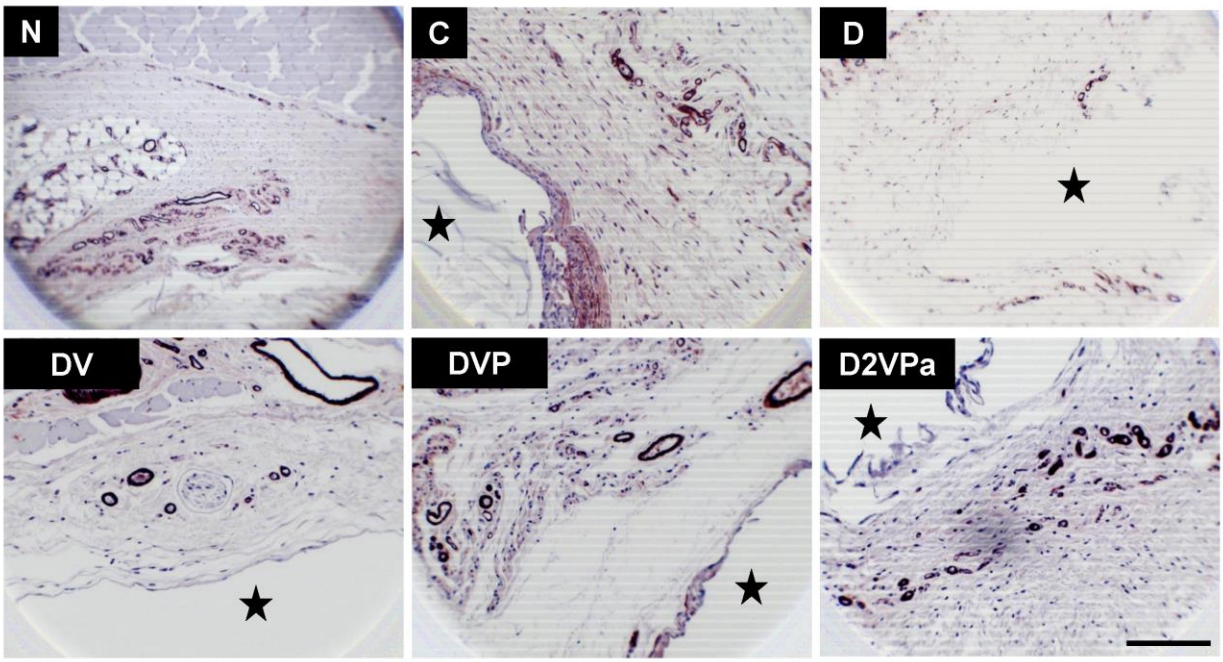

Figure 4.3. Anti-sma-stained tissue sections showing normal tissue (N) and composites C, D, DV, DVP, and D2VPa. Star denotes implant location. Magnification: 20x. Scale bar: 150 μm.

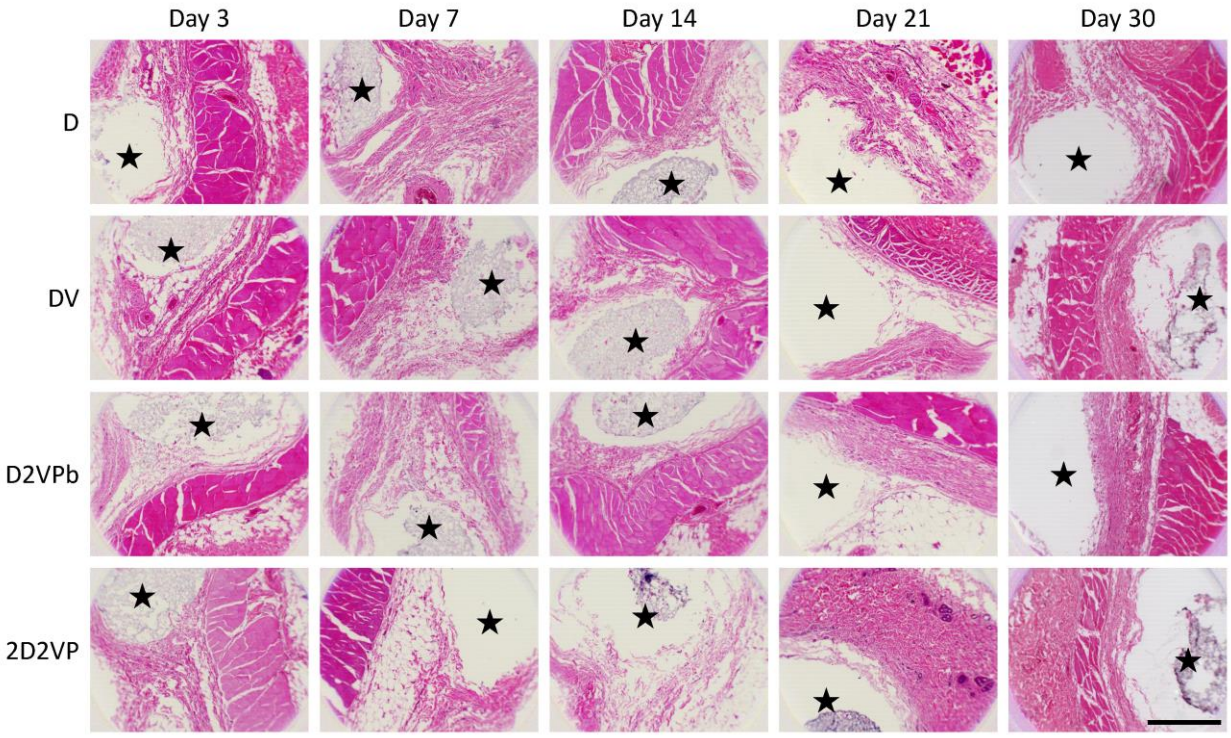

Figure 4.4. H&E-stained tissue sections of composites D, DV, D2VPb, and 2D2VP at different time points following implantation. Star denotes implant location. Magnification: 10x. Scale bar: 500 μm.

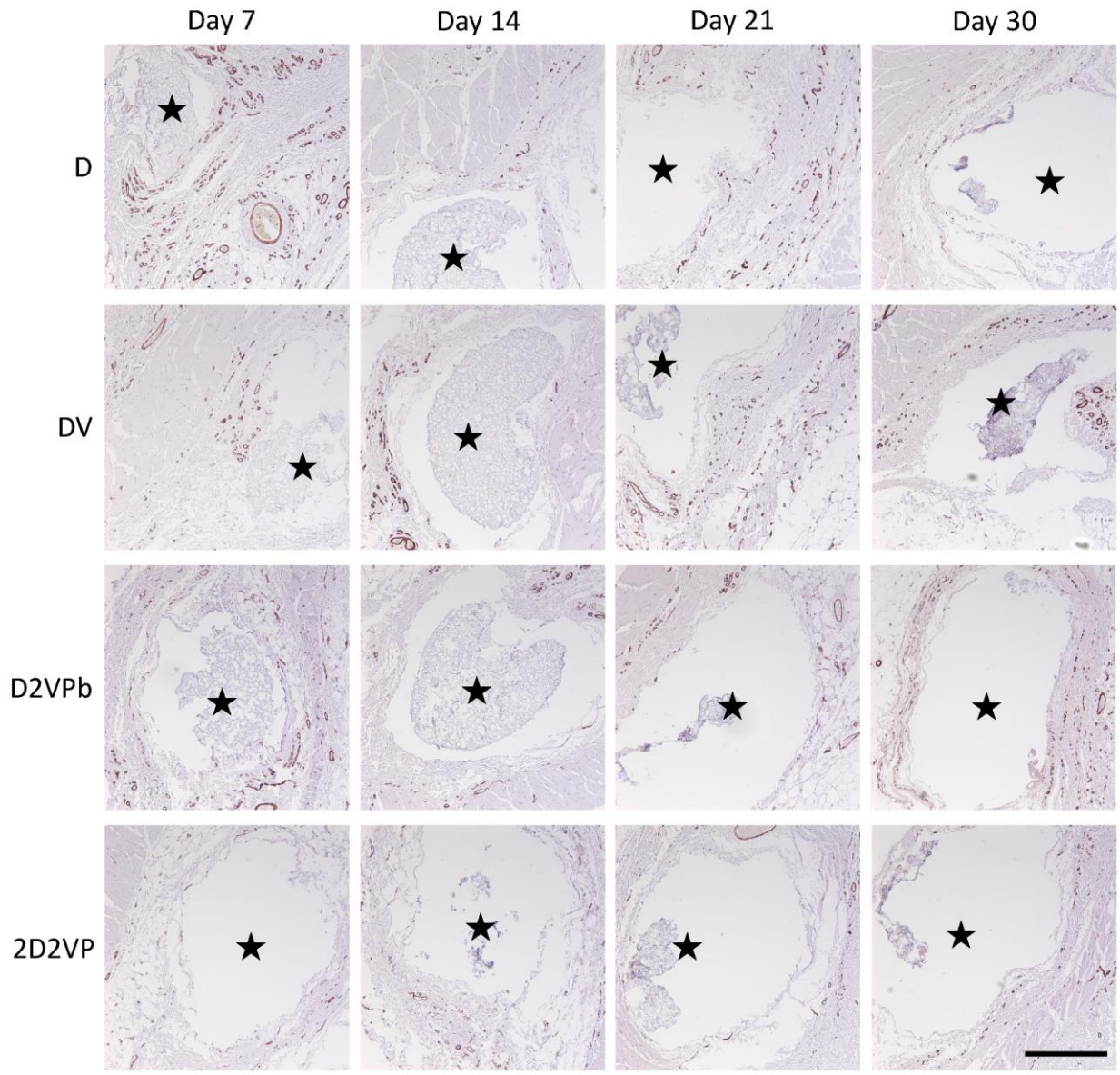

Figure 4.5. Anti-sma-stained tissue sections of composites D, DV, D2VPb, and 2D2VP at different time points following implantation. Star denotes implant location. Magnification: 10x. Scale bar: 500 μm.

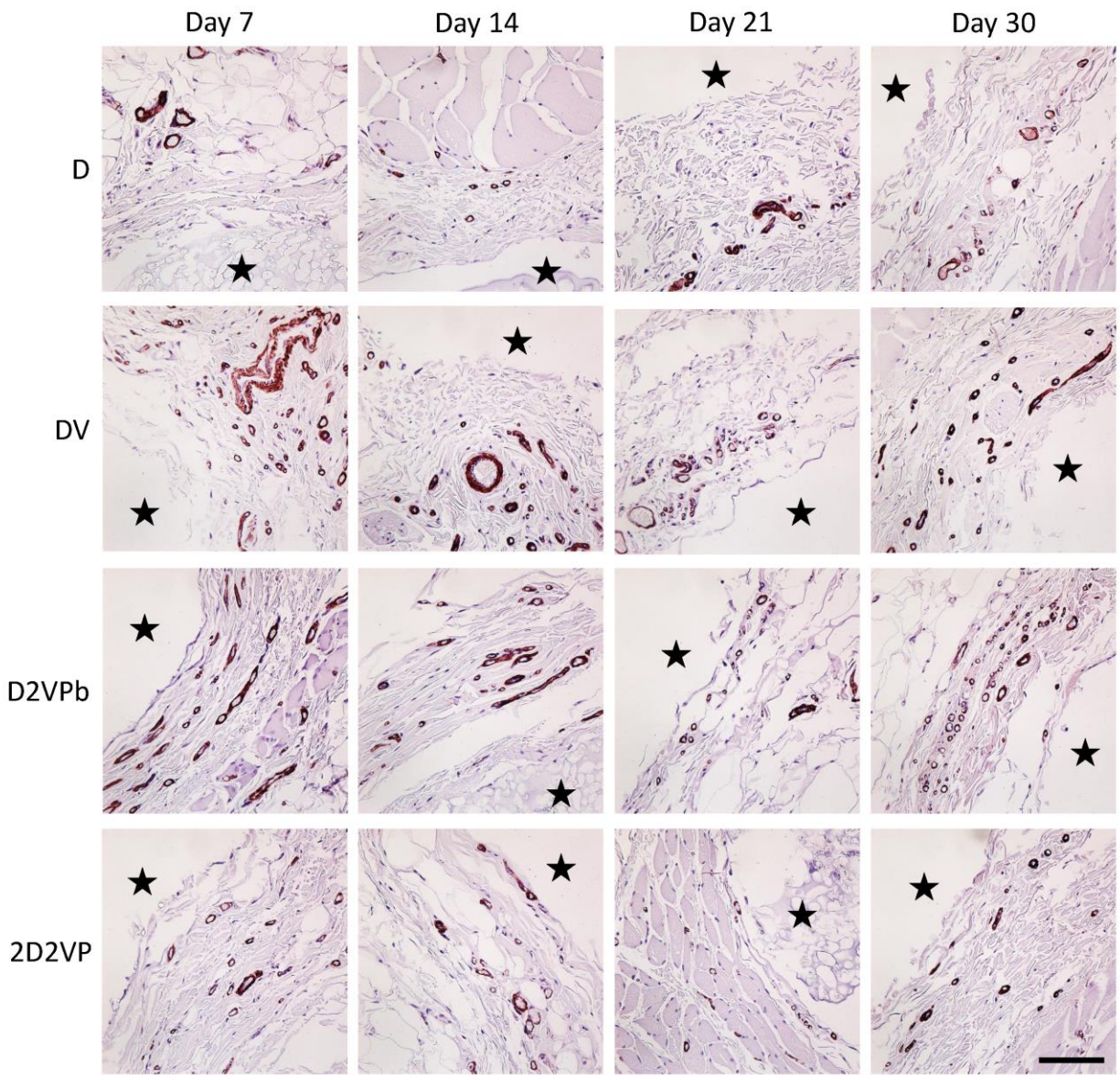

Figure 4.6. Anti-sma-stained tissue sections of composites D, DV, D2VPb, and 2D2VP at different time points following implantation. Star denotes implant location. Magnification: 140x. Scale bar: 100 μm.

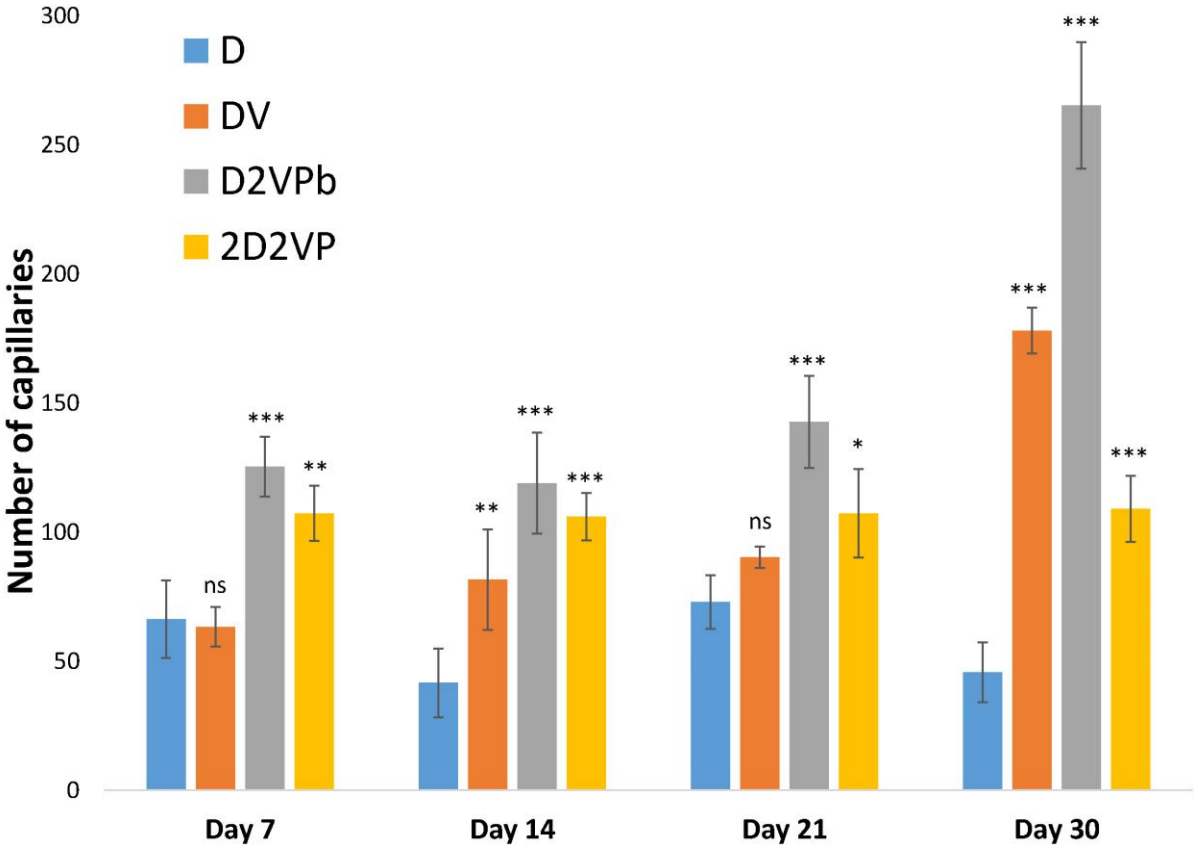

Figure 4.7. Capillary density within a 200 μm distance from the implant surface for composites D, DV, D2VPb and 2D2VP (mean ± SD, n=3).

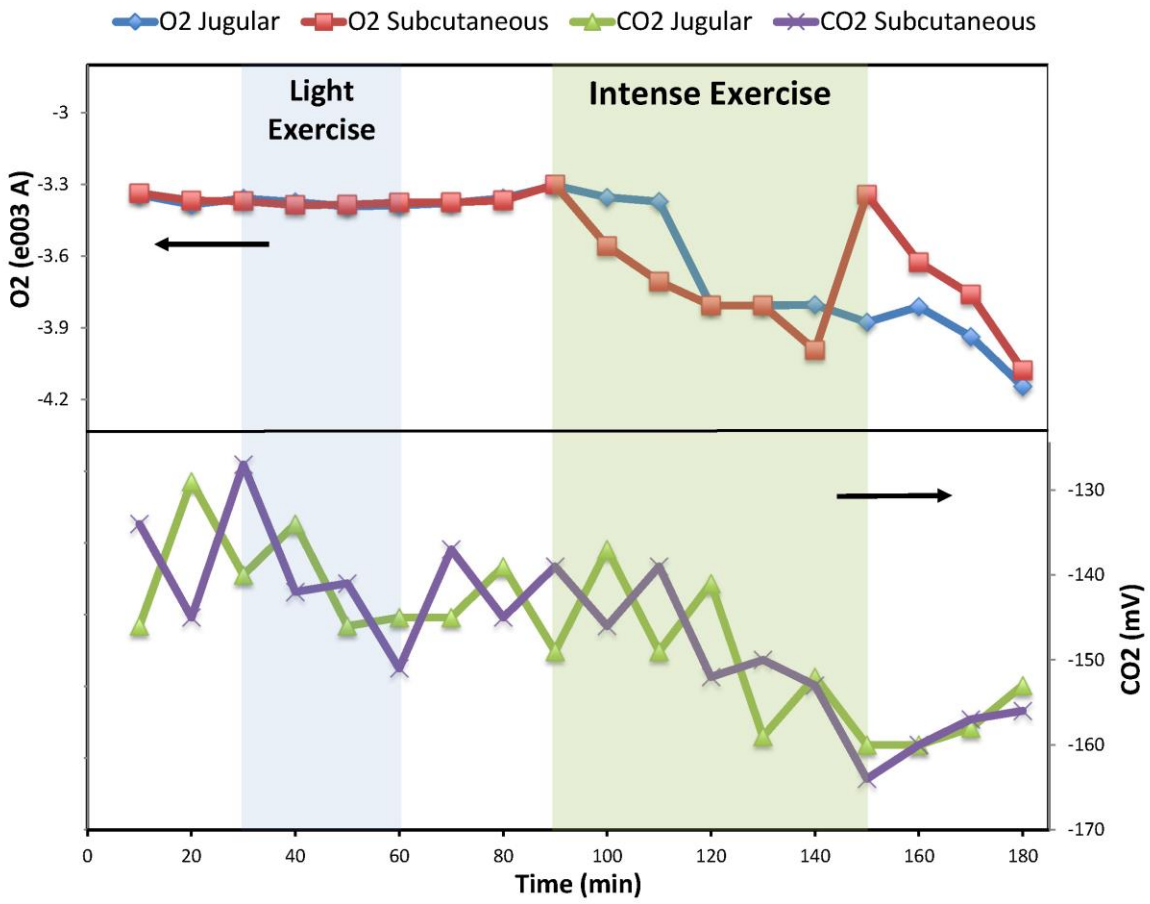

Figure 5.1. Effect of light and intense exercise on oxygen and carbon dioxide levels in the blood and subcutaneous tissue. Areas shaded blue and green indicate light and intense exercise, respectively, and unshaded areas indicate periods of inactivity (rest or recovery). The top panel displays oxygen level changes and the bottom panel carbon dioxide changes in the dialysate. Arrows indicate y axis. Oxygen levels did not respond to light exercise but only during intense exercise. Carbon dioxide levels responded to both light and intense exercise, but showed highly unstable readings.

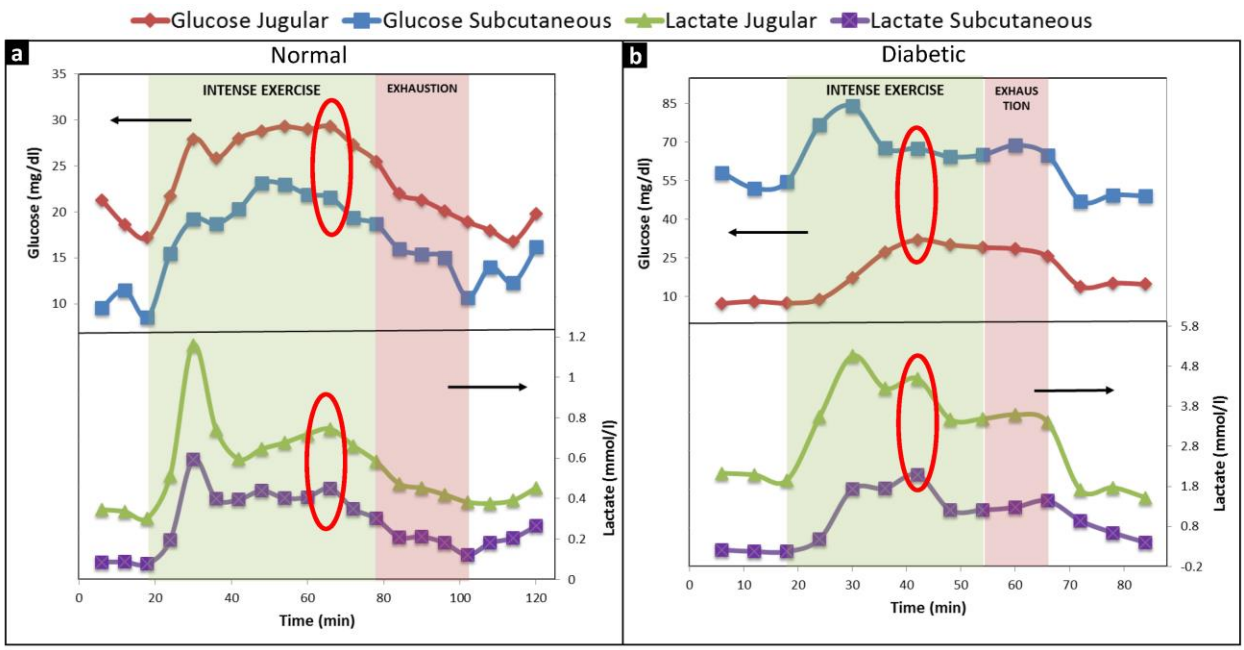

Figure 5.2. Effect of intense exercise and exhaustion on glucose and lactate levels in the blood and subcutaneous tissue. Areas shaded green and red indicate periods of intense exercise and exhaustion, respectively. Exhaustion was defined as the time when the animal could not keep up with the exercise and the running speed needed to be adjusted. Unshaded areas indicate periods of inactivity (rest or recovery). Arrows indicate y axis. Top panels show glucose and lower panels show lactate changes in the dialysate. Panel *a* shows representative graph from a normal rat and panel *b* from a diabetic rat. Changes in analyte trends precede the onset of exhaustion (red ovals). These are clearer in lactate trends for both normal and diabetic rats.

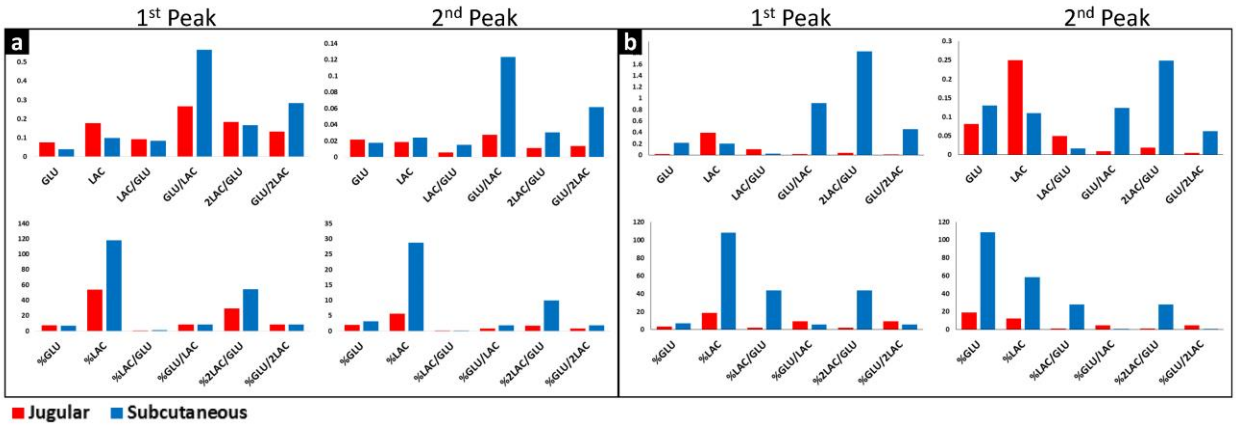

Figure 5.3. Slope changes for various biomarker combinations of glucose (GLU) and lactate (LAC). All ratios are molar and the percentile changes are calculated based on the baseline measurements before the commencement of the exercise. The first peak represents metabolic changes from rest to activity and the second peak metabolic changes that precede exhaustion (predictive). Panel *a* shows representative results from a normal rat and panel *b* from a diabetic rat.

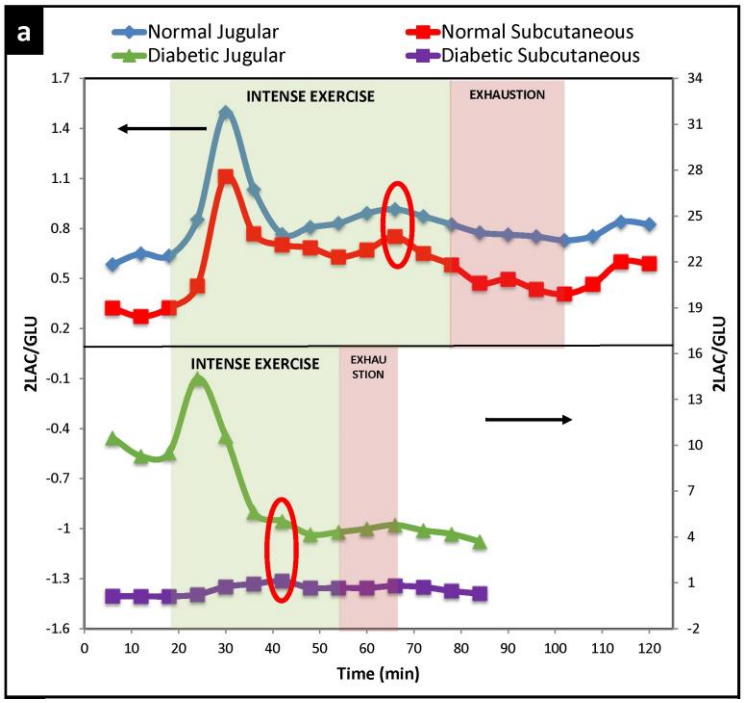

Figure 5.4a. Effect of intense exercise and exhaustion on the biomarker 2LAC/GLU (molar ratio of lactate and glucose multiplied by 2). Areas shaded green and red indicate periods of intense exercise and exhaustion, respectively. Exhaustion was defined as the time when the animal could not keep up with the exercise and the running speed needed to be adjusted. Unshaded areas indicate periods of inactivity (rest or recovery). Arrows indicate y axis. Red ovals indicate the exhaustion-prediction point. The top panel shows representative results from a normal rat and the bottom panel from a diabetic rat. 2LAC/GLU is the optimum biomarker for detecting metabolic changes in the subcutaneous tissue predictive of imminent exhaustion. The results are less clear in the diabetic rat; please note that diabetic rats did not receive insulin treatment, and the baseline glucose was high. This likely interfered with the biomarkers.

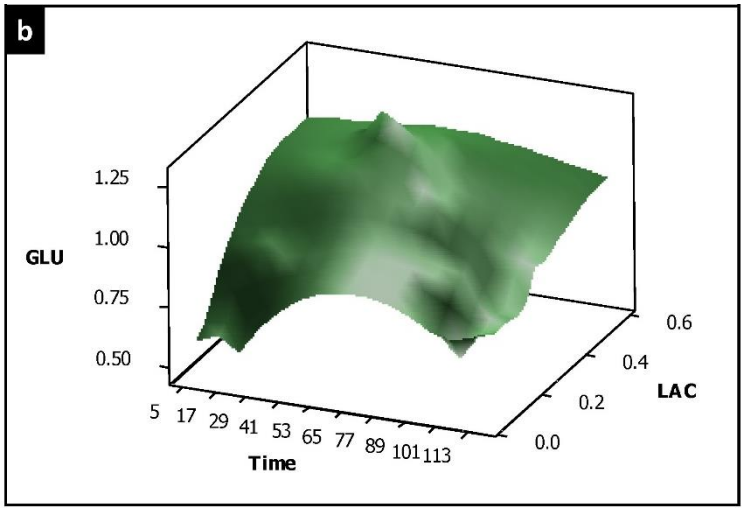

Figure 5.4b. 3D representation of glucose and lactate changes during intense exercise and exhaustion in a normal rat. This plot reveals the interdependence of glucose and lactate that can be extrapolated to evaluate the metabolic flexibility (the ability to transition from aerobic to anaerobic energy utilization). The peak in the graph indicates metabolic changes predictive of exhaustion.

Appendix II – Tables

Table 2.1. Implant composition and size.

Implant	Microspheres	PLGA per ml PVA solution (mg)	Length (mm)
Control	Blank	75	7
R	1M	75	7
R150	1M	150	7
R9	1M	75	9
R11	1M	75	11
R2W	2W	150	7

Table 2.2. Physical properties of PLGA microspheres. Results are average values ± SD (n=3).

Microspheres	Extend of polymer degradation	PLGA MW (g/mol)	Mean particle size (um ± SD)	Drug loading (% w/w ± SD)
1M	1 month	25,000	49.18 ± 5.84	10.54 ± 0.34
2W	2 weeks	12,000	38.95 ± 1.94	11.86 ± 0.13

Table 4.1. Microsphere content in the composites

Composite	Microspheres (mg) per ml PVA solution			
	D_MS	V_MS	P_MS	VP_MS
C	-	-	-	-
D	75	-	-	-
DV	75	50	-	-
DVP	75	50	50	-
DV2P	75	25	50	-
D2VPa	75	50	25	-
D2VPb	75	-	-	50
2DVP	100	-	-	50

Table 4.2. Microsphere characterization

Formulation	Drug Loading			Particle Size (μm)
	Dexamethasone (% w/w)	VEGF (ng/mg)	PDGF (ng/mg)	
D_MS	10.54 ± 0.34	-	-	39.63 ± 5.44
V_MS	-	3.19 ± 0.37	-	33.07 ± 5.46
P_MS	-	-	3.86 ± 0.22	41.69 ± 7.80
VP_MS	-	3.32 ± 0.17	1.91 ± 0.16	38.37 ± 4.46